Electronic Supplementary Material (ESI) for ChemComm.

Supporting Information

Accessing cationic tetrylene-nickel(0) systems featuring donor-acceptor E-Ni triple bonds (E = Ge, Sn)

Philip M. Keil,[a] Terrance J. Hadlington*,[a]

[a] Lehrstuhl für anorganische Chemie mit Schwerpunkt neue Materialien, Technische Universität München, Lichtenbergstraße 4, 85747 Garching

1. Experimental methods and data

General considerations. All experiments and manipulations were carried out under dry oxygen free argon atmosphere using standard Schlenk techniques or in a MBraun inert atmosphere glovebox containing an atmosphere of high purity argon. THF was dried by distillation over a sodium/benzophenone mixture and stored over activated 4Å mol sieves. C_6D_6 was dried, degassed and stored over a potassium mirror. All other solvents were dried over activated 4Å mol sieves. ^{SiiP}DippK (^{SiiP}DippK = ($^{i}Pr_3Si$)DippNK; Dipp = 2,6-$^{i}Pr_2$-C_6H_3),[1] Na[BAr^F_4] (Ar^F = 3,5-CF_3-C_6H_3),[2] and Ni(cod)$_2$ [3] were synthesized according to known literature procedures. All other reagents were used as received. NMR spectra were recorded on a Bruker AV 400 Spectrometer. The ^{1}H and ^{13}C{^{1}H} NMR spectra were referenced to the residual solvent signals as internal standards. ^{29}Si{^{1}H} NMR spectra were externally calibrated with $SiMe_4$. ^{31}P{^{1}H} NMR spectra were externally calibrated with H_3PO_4. ^{119}Sn{^{1}H} NMR spectra were externally calibrated with $SnMe_4$. Liquid Injection Field Desorption Ionization Mass Spectrometry (LIFDI-MS) was measured directly from an inert atmosphere glovebox with a Thermo Fisher Scientific Exactive Plus Orbitrap equipped with an ion source from Linden CMS.[4] Absorption spectra (UV/vis) were recorded on an Agilent Cary 60 UV/vis spectrophotometer. For the ammonia experiments ammonia 5.0 was used. Elemental analyses (C, H, N) were performed with a combustion analyzer (elementar vario EL, Bruker).

^{SiiP}DippGeCl, 1. A solution of ^{SiiP}DippK (1.60 g, 4.30 mmol) in 20 mL THF was added dropwise to a stirring solution of $GeCl_2$·dioxane (1.00 g, 4.30 mmol) in 10 mL THF at -78°C, and subsequently allowed to warm to RT, resulting in the formation of a pale-yellow solution. All volatiles were removed *in vacuo* and the residue extracted in 20 mL of pentane. The solution was concentrated and stored at -30°C for 16h to yield colorless crystals suitable for X-ray diffraction analysis (1.42 g, 3.22 mmol, 75%).

^{1}H NMR (C_6D_6, 400 MHz, 298 K): δ = 0.99 (d, 18H, $^3J_{HH}$ = 7.5 Hz, Si-Pr^i-C*H*$_3$), 1.25 (m, 15H, Dipp-Pr^i-C*H*$_3$, Si-Pr^i-C*H*), 3.14 (hept, 2H, $^2J_{HP}$ = 6.9 Hz, Dipp-Pr^i-C*H*), 7.12 (m, 3H, Ar-C*H*).
^{13}C{^{1}H} NMR (C_6D_6, 101 MHz, 298 K): δ = 13.1 (Si-Pr^i-*C*H), 18.8 (Si-Pr^i-*C*H$_3$), 24.0 (Dipp-Pr^i-*C*H$_3$), 26.4 (Dipp-Pr^i-*C*H$_3$), 28.2 (Dipp-Pr^i-*C*H), 124.3, 125.9, 142.4, 143.2 (Ar-*C*).
^{29}Si{^{1}H} NMR (C_6D_6, 99 MHz, 298 K): δ = 12.8 (s, *Si*-Pr^i).
MS/LIFDI-HRMS found (calcd.) m/z: 406.1996 (406.1980) for $[M\text{-}Cl]^+$.

[^{SiiP}DippSnCl]$_2$, 2. The procedure for the synthesis of **1** was followed using **^{SiiP}DippK** (4.00 g, 10.76 mmol) and $SnCl_2$ (2.04 g, 10.76 mmol). Compound **2** was isolated as colorless crystals suitable for X-ray diffraction analysis from a concentrated pentane solution stored at -32°C after 16h (3.80 mg, 7.81 mmol, 73%).

N.B. On one occasion, a low yield of crystalline **2·KCl** was obtained *via* this procedure, which is formally the KCl adduct of **2**. Its X-ray crystal structure is shown Figure S32. No further data was obtained for this compound.

^{1}H NMR (C_6D_6, 400 MHz, 298 K): δ = 1.11 (d, 36H, $^{3}J_{HH}$ = 7.5 Hz, Si-Pr^{i}-C*H*$_3$), 1.28 (m, 30H, Dipp-Pr^{i}-C*H*$_3$, Si-Pr^{i}-C*H*), 3.51 (hept, 4H, $^{2}J_{HP}$ = 6.8 Hz, Dipp-Pr^{i}-C*H*), 7.10 (m, 6H, Ar-C*H*).

^{13}C{^{1}H} NMR (C_6D_6, 101 MHz, 298 K): δ = 14.3 (Si-Pr^{i}-*C*H), 19.4 (Si-Pr^{i}-*C*H$_3$), 24.2 (Dipp-Pr^{i}-*C*H$_3$), 27.6 (Dipp-Pr^{i}-*C*H), 27.9 (Dipp-Pr^{i}-*C*H$_3$), 124.1, 125.2, 142.7, 145.9 (Ar-*C*).

^{29}Si{^{1}H} NMR (C_6D_6, 99 MHz, 298 K): δ = 9.0 (s, *Si*-Pr^{i}).

^{119}Sn NMR (C_6D_6, 149 MHz, 298K): δ = 232 (s, N-*Sn*-Cl).

MS/LIFDI-HRMS found (calcd.) m/z: 452.1787 (452.1790) for [M-iPr$_3$SiNDippSnCl-Cl]$^{+}$.

Anal. calcd. for $C_{21}H_{38}ClNSiSn$: C, 51.82%; H, 7.87%; N, 2.88%; found: C, 50.81%; H, 7.44%; N, 2.92%. Repeated element analysis gave variable but consistently low values for C, possibly due to Si-carbide formation.

[(SiiPDipp)(Cl)Ge·Ni^{0}(PPh$_3$)$_2$], 3. A toluene solution of **1** (300 mg, 0.68 mmol) and PPh_3 (535 mg, 2.04 mmol) was added dropwise to a toluene solution of $Ni(cod)_2$ (187 mg, 0.68 mmol) at -40°C and stirred for 30 min. The mixture was filtrated, layered with pentane, and stored at -32°C. After 24 h a few orange crystals of **3** were isolated suitable for X-ray diffraction analysis (see Figure S33). No further data on **3** could be collected due to insufficient quantity and instability of the compound.

[SiiPDippGe·Ni^{0}(PPh$_3$)$_3$][BAr$^{F}_4$], 4. Compound **1** (272 mg, 0.62 mmol), $Ni(cod)_2$ (170 mg, 0.62 mmol), PPh_3 (485 mg, 1.85 mmol) and Na[BAr$^{F}_4$] (547 mg, 0.62 mmol) were mixed together in a Schlenk flask and cooled to -78°C. 10 mL of toluene was slowly added to the flask and the resulting reaction mixture was slowly warmed to RT overnight, leading to a dark purple precipitate within a dark red solution. All volatiles were removed *in vacuo* and the residue was extracted with fluorobenzene. The deep purple solution was concentrated to approximately 2 mL and 5 mL of pentane were slowly added to the flask while constantly shaking the flask. The resulting solution was stored at -32°C overnight yielding a crop of dark purple crystals. The remaining solution was removed, and the crystals subsequently washed with toluene and pentane and dried *in vacuo* yielding **4** (614 mg, 0.29 mmol, 47%) as a purple crystalline powder. Deep red-purple crystals which were suitable for X-Ray diffraction analysis were obtained from a concentrated fluorobenzene solution layered with pentane at RT after 24h.

N. B. Dissolving the pure compound in THF-d_8 resulted in two species being present in the NMR spectra, which we hypothesise is due to reversible dissociation of one PPh_3 ligand from Ni^{0}. Even though two species were present, the integrals of the aromatic and the

aliphatic in the ^{1}H NMR matched for 3 equivs. of PPh_3 being present. Addition of 2 equivs. of PPh_3 to the NMR tube led to the formation of one species. The spectra with added PPh_3 are described here; both sets of spectra are shown later in the Supporting Information.

^{1}H NMR (THF-d_8, 400 MHz, 298 K): δ = 0.80 (m, 24 H, Si-Pr^{i}-C*H*$_3$/Dipp-Pr^{i}-C*H*$_3$), 0.98 (hept, 3 H, $^{3}J_{HH}$ = 7.5 Hz, Si-Pr^{i}-C*H*), 1.20 (d, 6 H, $^{3}J_{HH}$ = 6.7 Hz, Dipp-Pr^{i}-C*H*$_3$), 3.23 (hept, 2H, $^{3}J_{HH}$ = 6.7 Hz, Dipp-Pr^{i}-C*H*), 7.26 (m, 108 H, Ar-C*H*), 7.60 (s, 4H, Ar$_{BArF}$-*H*$_{para}$), 7.83 (s, 8H, Ar$_{BArF}$-*H*$_{ortho}$).

^{13}C{^{1}H} NMR (THF-d_8, 101 MHz, 298 K): δ = 15.0 (Si-Pr^{i}-*C*H), 18.8 (Si-Pr^{i}-*C*H$_3$), 23.6 (Dipp-Pr^{i}-*C*H$_3$), 28.6 (Dipp-Pr^{i}-*C*H$_3$), 29.0 (Dipp-Pr^{i}-*C*H), 118.3, 121.5, 124.3, 126.1, 126.9, 128.9, 129.0, 129.4, 129.5, 129.6, 129.9, 130.2, 130.6, 131.4, 131.7, 133.3, 134.9, 135.7, 140.7, 148.2, 162.2, 162.7, 163.1, 163.6 (Ar-*C*).

^{31}P{^{1}H} NMR (THF-d_8, 162 MHz, 298 K): δ = 37.2 (s, Ni-*P*Ph$_3$).

^{29}Si{^{1}H} NMR (THF-d_8, 79 MHz, 298 K): δ = 17.3 (s, Pr$^{i}_3$-*Si*).

λ$_{max}$, nm (***ε***, Lmol^{-1}cm^{-1}): 323 (9384).

MS/LIFDI-HRMS found (calcd.) m/z: 988.3169 (988.3162) for [M-PPh$_3$]$^{+}$.

Anal. calcd. for $C_{107}H_{95}BF_{24}GeNNiP_3Si$: C, 60.79%; H, 4.53%; N, 0.66%; found: C, 60.31%; H, 4.54%; N, 0.75%. Repeated element analysis gave variable but consistently low values for C, possibly due to Si-carbide/Ni-carbide formation

[^{SiiP}DippSn·Ni^{0}(PPh$_3$)$_3$][BAr$^{F}_4$], 5. Compound **2** (300 mg, 0.62 mmol), Ni(cod)$_2$ (170 mg, 0.62 mmol), PPh_3 (485 mg, 1.85 mmol) and Na[BAr$^{F}_4$] (546 mg, 0.62 mmol) were mixed together in a Schlenk flasked and cooled to -78°C. 10 mL of toluene was slowly added to the flask and the resulting reaction mixture was slowly warmed to RT overnight leading to a dark blue precipitate within a light yellow solution. All volatiles were removed *in vacuo* and the residue was exctracted with fluorobenzene. The deep black solution was concentrated to approximately 2 mL and 5 mL of pentane were slowly added to the flask while constantly shaking the flask. The resulting solution was stored at -32°C overnight yielding a crop of dark blue crystals. The remaining solution was removed, and the crystals subsequently washed with toluene and pentane and dried *in vacuo* yielding **5** (595 mg, 0.28 mmol, 45%) as a blue crystalline powder. Dark blue-purple crystals which were suitable for X-Ray diffraction analysis were obtained from a concentrated fluorobenzene solution layered with pentane at RT after 24h.

^{1}H NMR (THF-d_8, 400 MHz, 233 K): δ = 0.83 (m, 24 H, Si-Pr^{i}-C*H*$_3$/Dipp-Pr^{i}-C*H*$_3$), 1.19 (d, 6 H, $^{3}J_{HH}$ = 6.5 Hz, Dipp-Pr^{i}-C*H*$_3$), 1.29 (m, 3 H, Si-Pr^{i}-C*H*), , 3.26 (hept, 2H, $^{3}J_{HH}$ = 6.3 Hz, Dipp-Pr^{i}-C*H*), 6.85 (m, 17 H, Ar-C*H*), 7.07 (t, 17 H, $^{3}J_{HH}$ = 7.5 Hz, Ar-C*H*), 7.18 (m, 2 H, Ar-C*H*), 7.41 (m, 12 H, Ar-C*H*), 7.65 (s, 4H, Ar$_{BArF}$-*H*$_{para}$), 7.85 (s, 8H, Ar$_{BArF}$-*H*$_{ortho}$).

$^{13}C\{^1H\}$ NMR (THF-d_8, 101 MHz, 233 K): δ = 15.5 (Si-Pr^i-*C*H), 18.8 (Si-Pr^i-*C*H$_3$), 23.6 (Dipp-Pr^i-*C*H$_3$), 28.5 (Dipp-Pr^i-*C*H$_3$), 28.8 (Dipp-Pr^i-*C*H), 115.9, 116.1, 118.3, 121.4, 124.1, 126.2, 126.4, 126.8, 128.3, 129.0, 129.6, 129.7, 129.8, 129.9, 130.2, 131.1, 131.2, 131.5, 134.4, 135.5, 135.9, 147.8, 162.2, 162.7, 163.2, 163.7 (Ar-*C*).

$^{31}P\{^1H\}$ NMR (THF-d_8, 162 MHz, 233 K): δ = 40.1 (s, Ni-*P*Ph$_3$).

^{119}Sn NMR (THF-d_8, 149 MHz, 233K): δ = 886 (s, N-*Sn*-Ni).

λ_{max}, nm (***ε***, Lmol^{-1}cm^{-1}): 350 (5520).

MS/LIFDI-HRMS found (calcd.) m/z: 726.2233 (726.2211) for [M-2PPh$_3$-CH-C$_3$H$_7$+10H]$^+$.

Anal. calcd. for $C_{107}H_{95}BF_{24}SnNNiP_3Si$: C, 59.50%; H, 4.43%; N, 0.65%; found: C, 57.67%; H, 4.20%; N, 0.74%. Repeated element analysis gave variable but consistently low values for C, possibly due to Si-carbide/Ni-carbide formation

N. B. It was not possible to obtain a $^{29}Si\{^1H]$ NMR spectrum of **5** due to the instability of this compound in THF-d_8.

Experiments with [SbF$_6$][PPh$_4$]:

4 (30 mg, 0.014 mmol) was mixed with [PPh$_4$][SbF$_6$] (8 mg, 0.024 mmol) in a NMR tube. The solids were mixed with 0.4 mL PhF and 0.1 mL C_6D_6 and sonicated for 5 min in an ultrasonic water bath. After 12 h the mixture changed color from blue to brown. ^1H and $^{31}P\{^1H\}$ NMR showed that **4** had been completely consumed. A mixture of many different products had formed including the protonated ligand ^{SiiP}DippH.

5 (30 mg, 0.014 mmol) was mixed with [PPh$_4$][SbF$_6$] (8 mg, 0.024 mmol) in a NMR tube. The solids were mixed with 0.4 mL PhF and 0.1 mL C_6D_6 and ultrasonicated for 5 min. After 12 h the mixture changed colour from blue to brown. ^1H and $^{31}P\{^1H\}$ NMR showed that **5** had completely been consumed. A mixture of many different products had formed including the protonated ligand ^{SiiP}DippH.

Ammonia experiments:

4 (30 mg, 0.014 mmol) was dissolved in 0.4 mL PhF and 0.1 mL C_6D_6 in a NMR tube. The NMR tube was filled with ammonia and then quickly closed and shaken. After 2 h the colour the reactions had changed from purple to brown. ^1H and $^{31}P\{^1H\}$ showed that **4** had completely been consumed. A mixture of many different products had formed including the protonated ligand ^{SiiP}DippH. Conducting at low-temperature had a similar outcome.

5 (30 mg, 0.014 mmol) was dissolved in 0.4 mL PhF and 0.1 mL C_6D_6 in a NMR tube. The NMR tube was filled with ammonia and then quickly closed and shaken. After 2 h the colour the reactions had changed from blue to brown. ^1H and $^{31}P\{^1H\}$ NMR showed that **5** had completely been consumed. A mixture of many different products had formed including the protonated ligand ^{SiiP}DippH. Conducting at low-temperature had a similar outcome.

NMR, Mass, and UV/vis Spectra

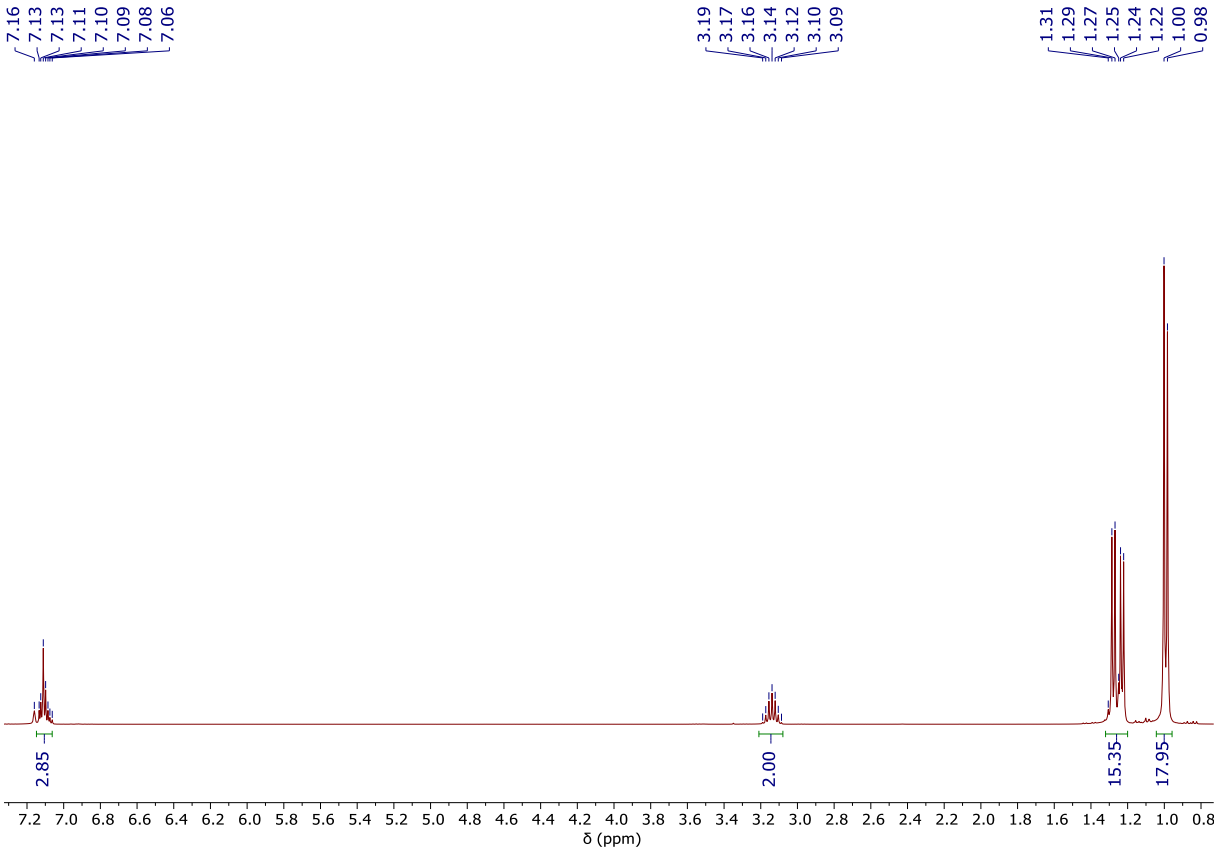

Figure S1. ^{1}H NMR spectrum of **1** as a solution in C_6D_6 at ambient temperature.

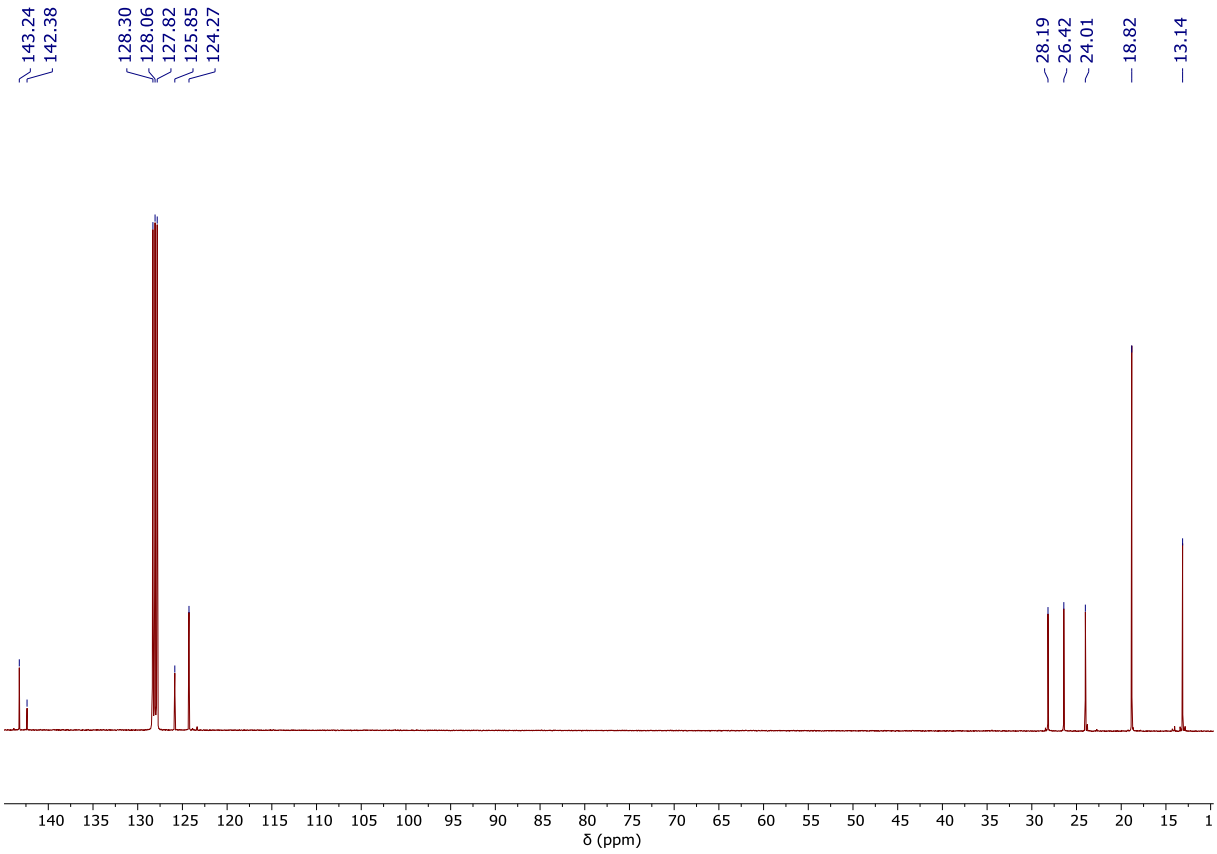

Figure S2. $^{13}C\{^{1}H\}$ NMR spectrum of **1** as a solution in C_6D_6 at ambient temperature.

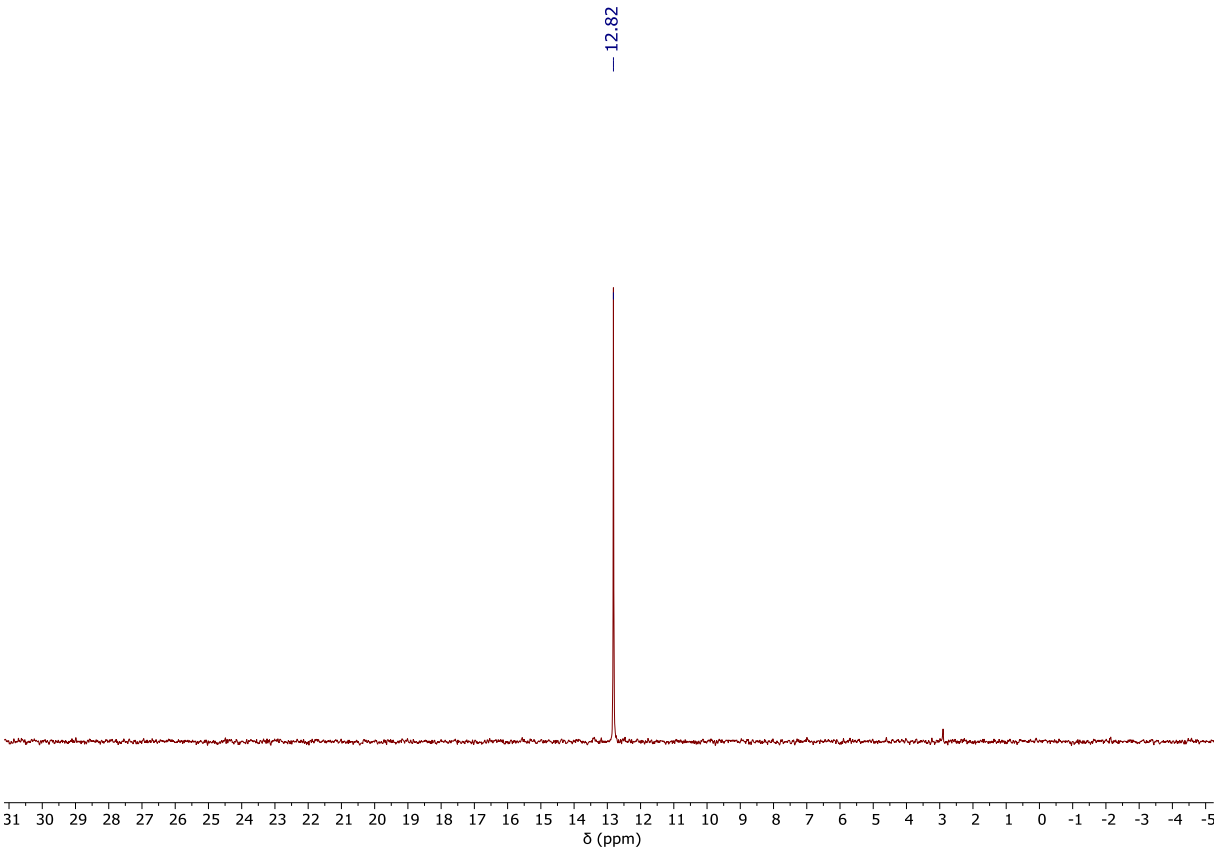

Figure S3. $^{29}Si\{^{1}H\}$ NMR spectrum of **1** as a solution in C_6D_6 at ambient temperature.

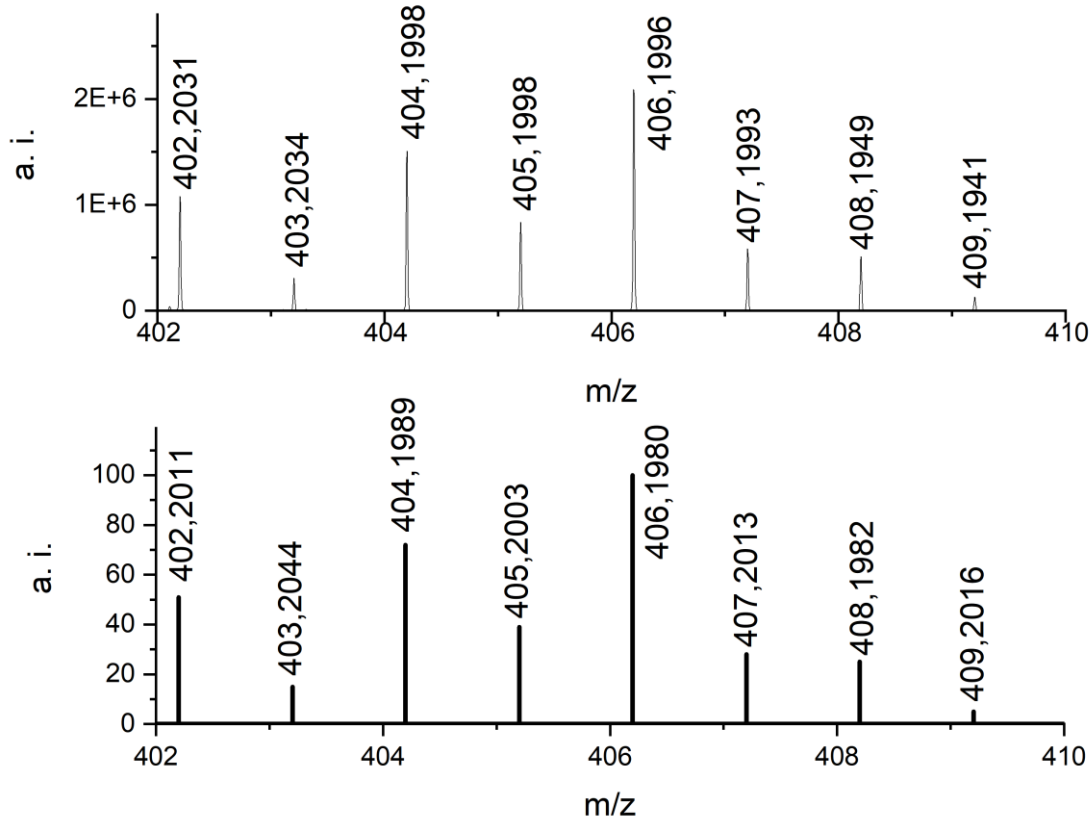

Figure S4. *Top*: Cutout from LIFDI/MS of **1**; *Bottom*: Calculated MS spectrum of **1**.

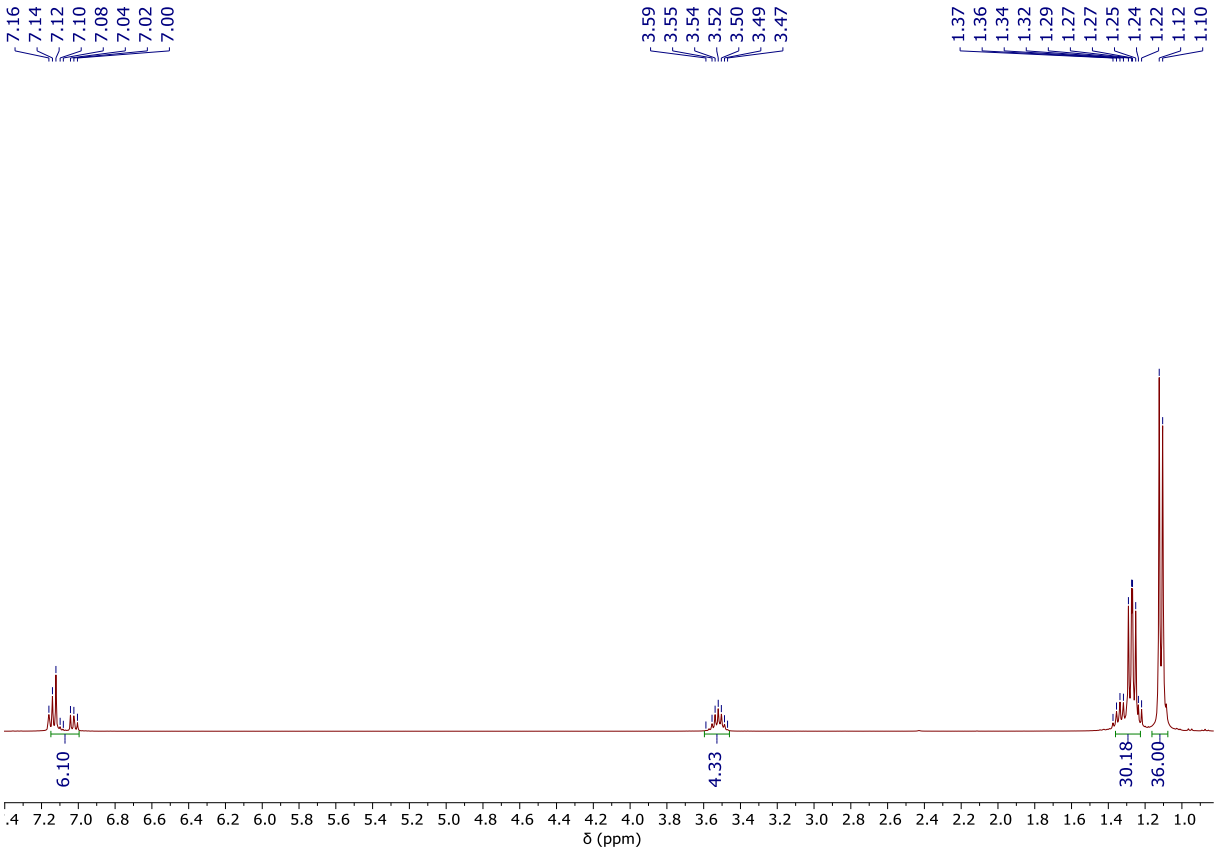

Figure S5. ^{1}H NMR spectrum of **2** as a solution in C_6D_6 at ambient temperature.

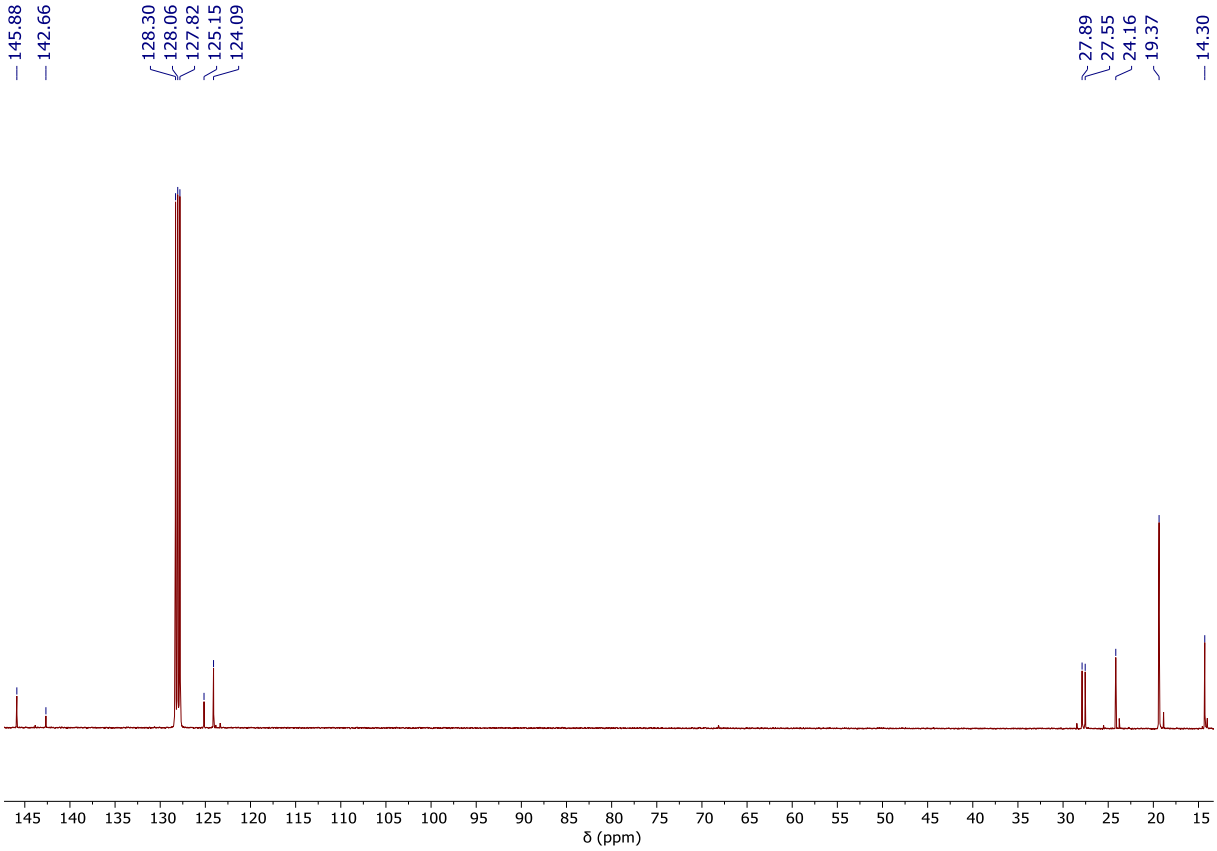

Figure S6. $^{13}C\{^{1}H\}$ NMR spectrum of **2** as a solution in C_6D_6 at ambient temperature.

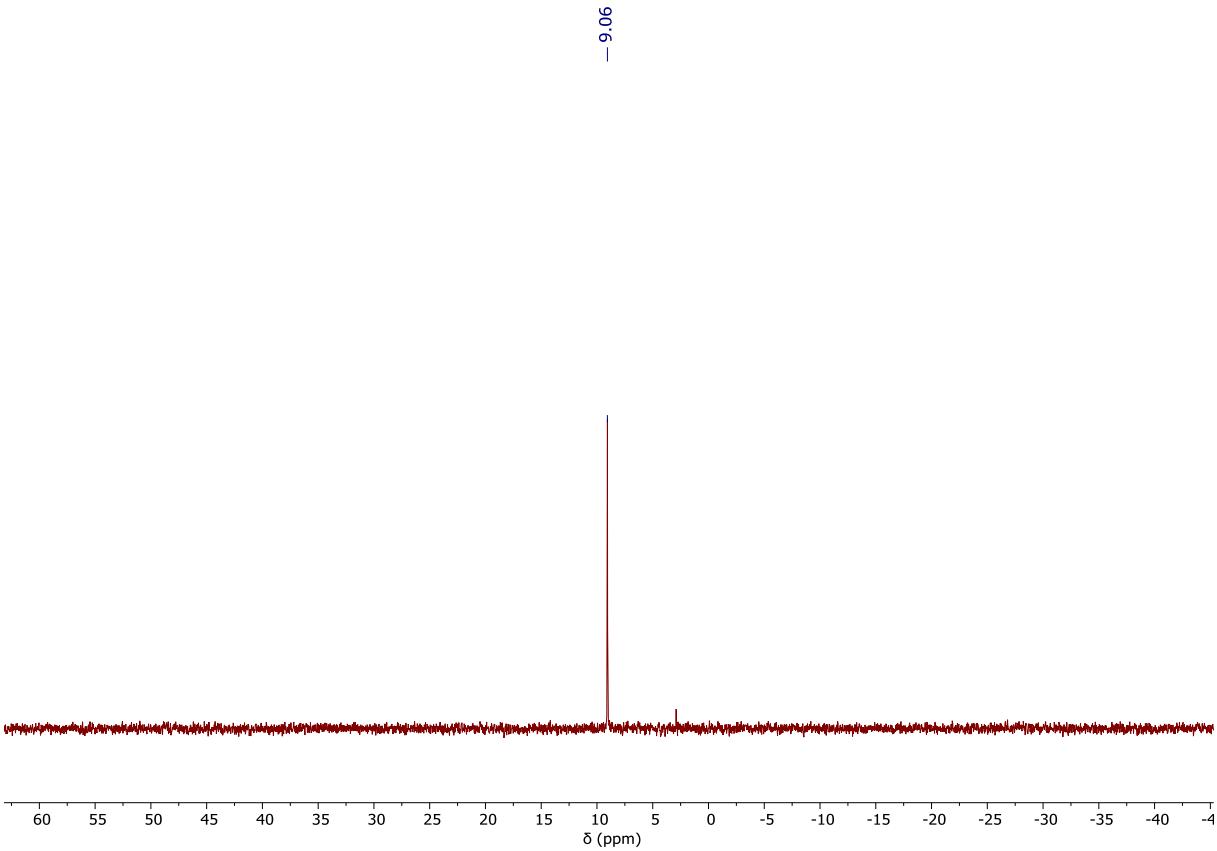

Figure S7. $^{29}Si\{^{1}H\}$ NMR spectrum of **2** as a solution in C_6D_6 at ambient temperature.

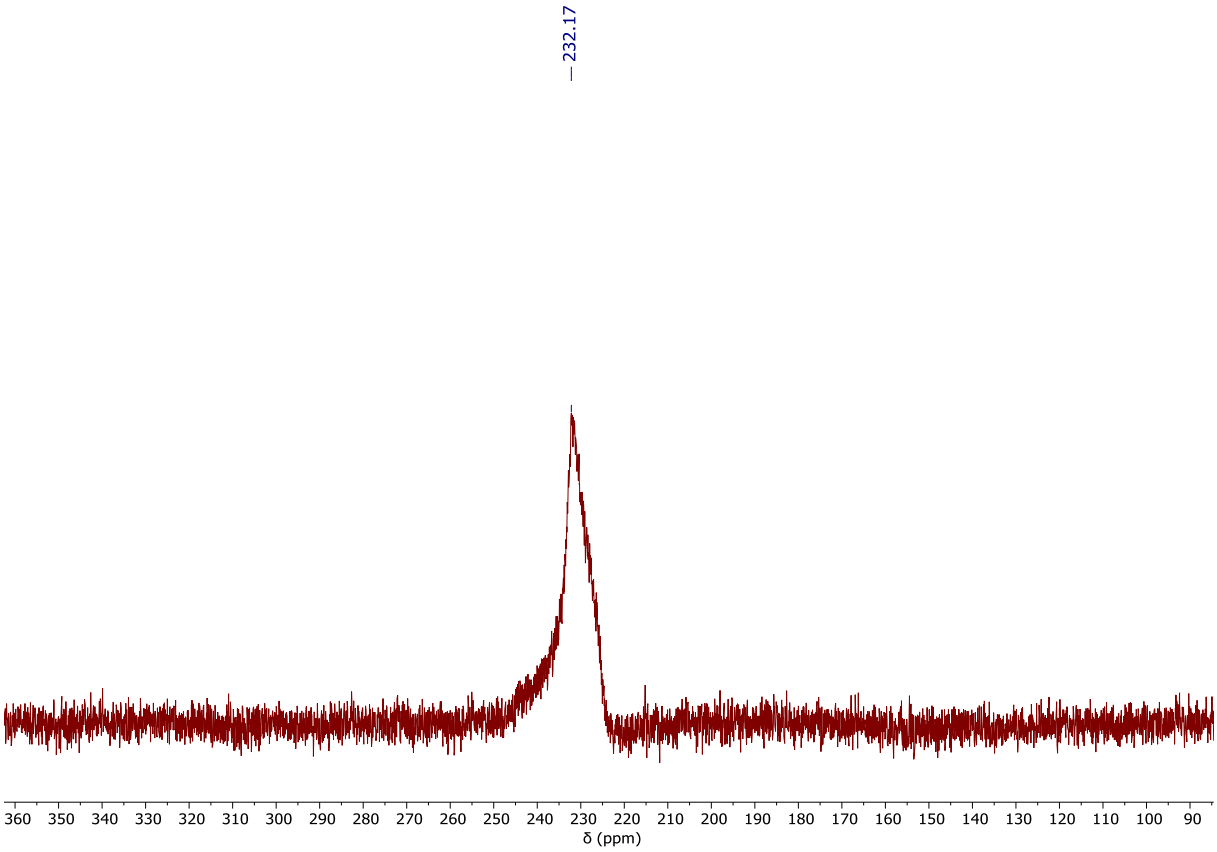

Figure S8. $^{119}Sn\{^{1}H\}$ NMR spectrum of **2** as a solution in C_6D_6 at ambient temperature.

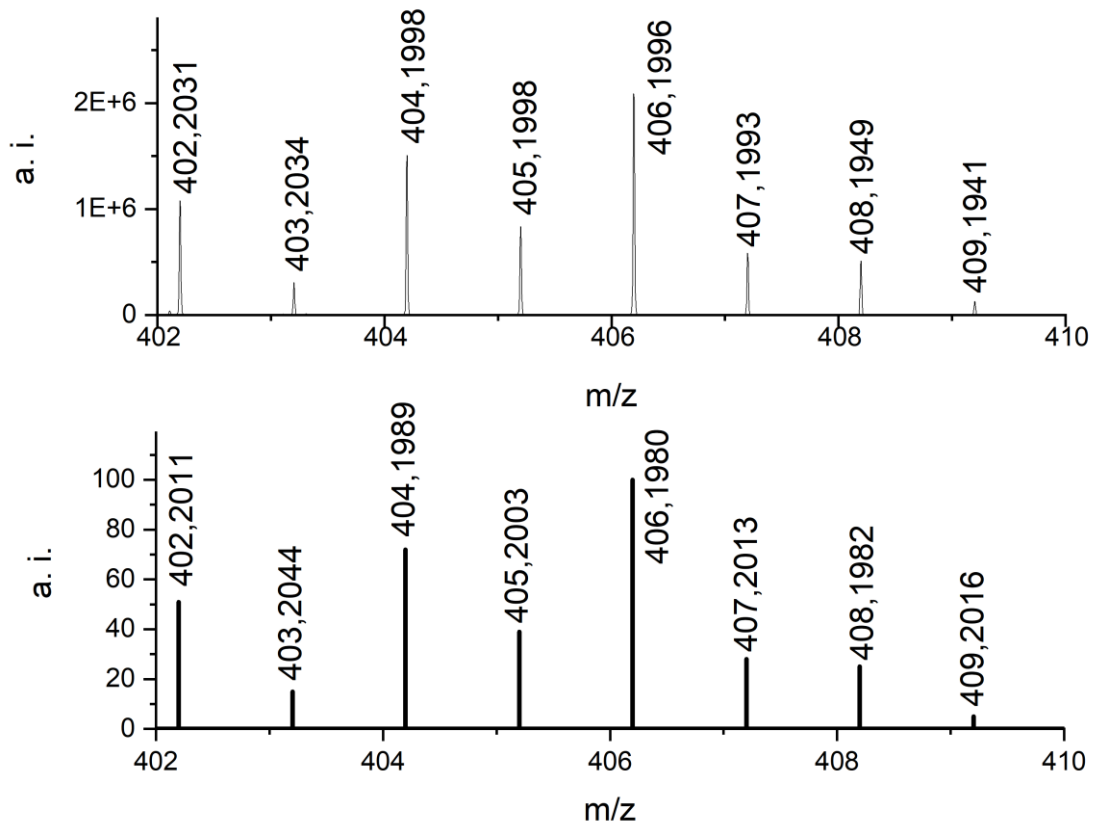

Figure S9. *Top*: Cutout from LIFDI/MS of **2**; *Bottom*: Calculated MS spectrum of **2**.

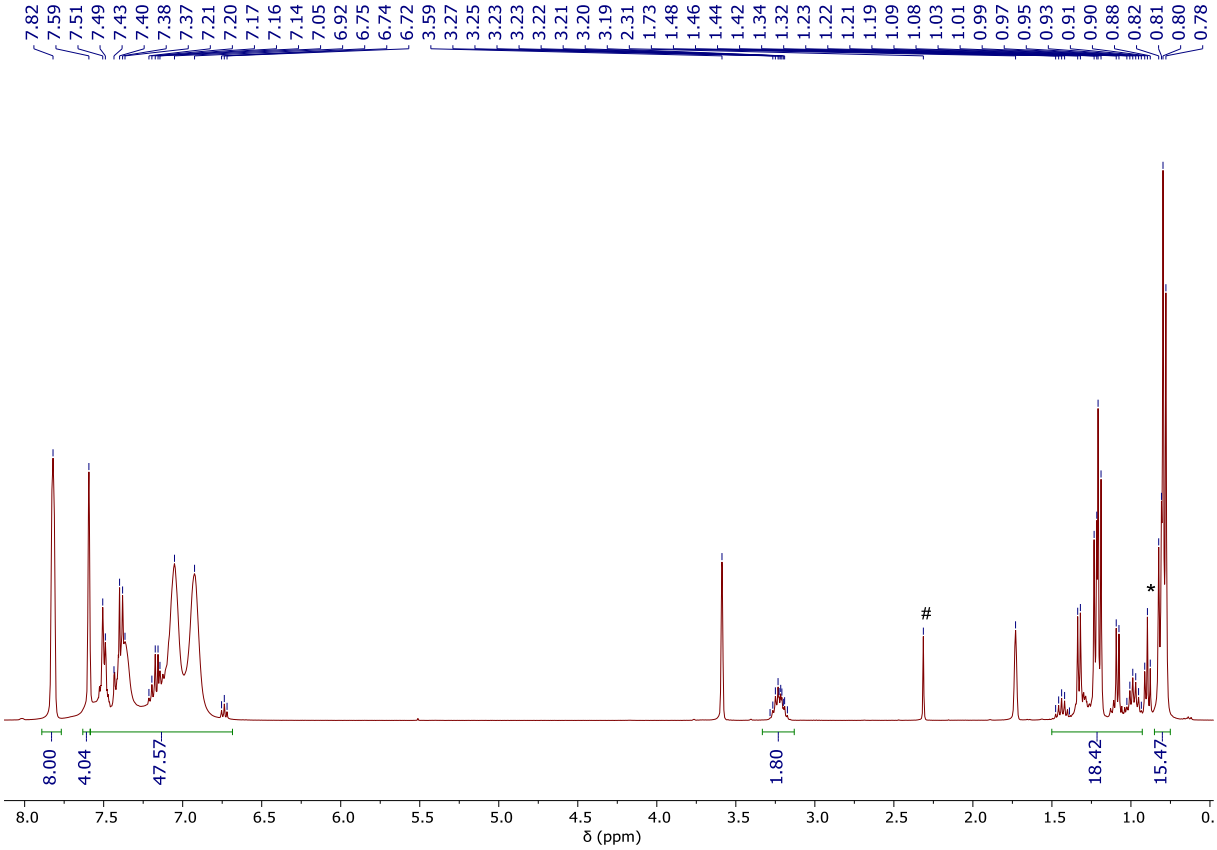

Figure S10. ^{1}H NMR spectrum of **4** as a solution in THF-d_8 at ambient temperature; * indicates presence of *n*-pentane; # indicates presence of toluene.

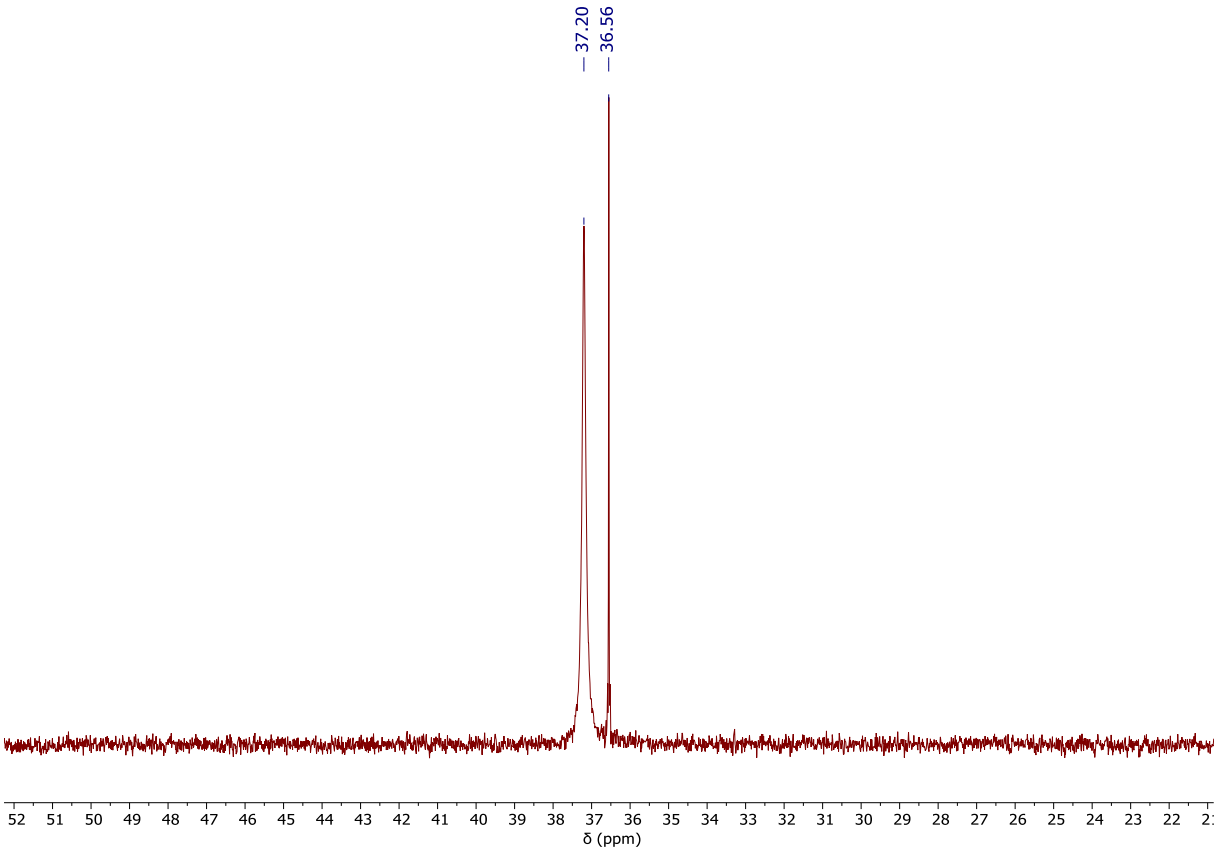

Figure S11. $^{31}P\{^{1}H\}$ NMR spectrum of **4** as a solution in THF-d_8 at ambient temperature.

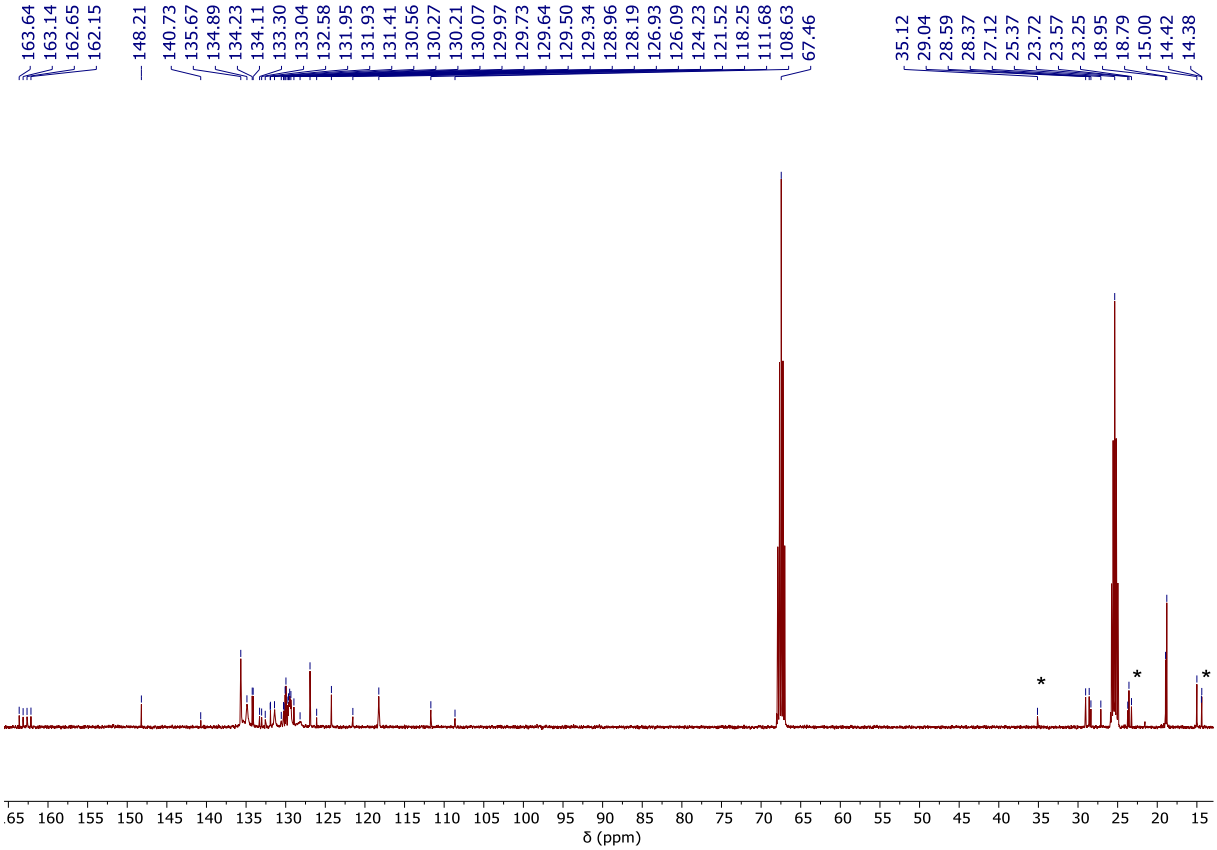

Figure S12. $^{13}C\{^{1}H\}$ NMR spectrum of **4** as a solution in THF-d_8 at ambient temperature; * indicates presence of n-pentane.

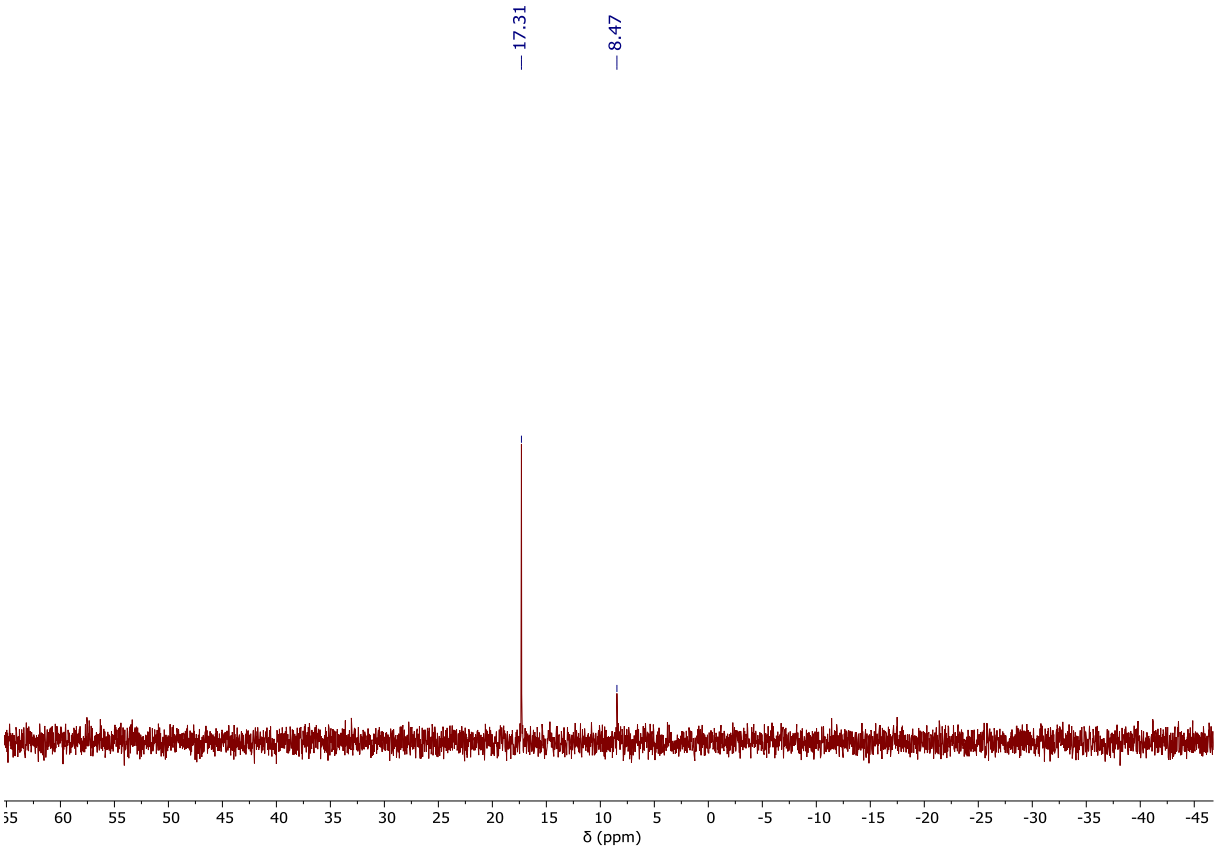

Figure S13. $^{29}Si\{^{1}H\}$ NMR spectrum of **4** as a solution in THF-d_8 at ambient temperature.

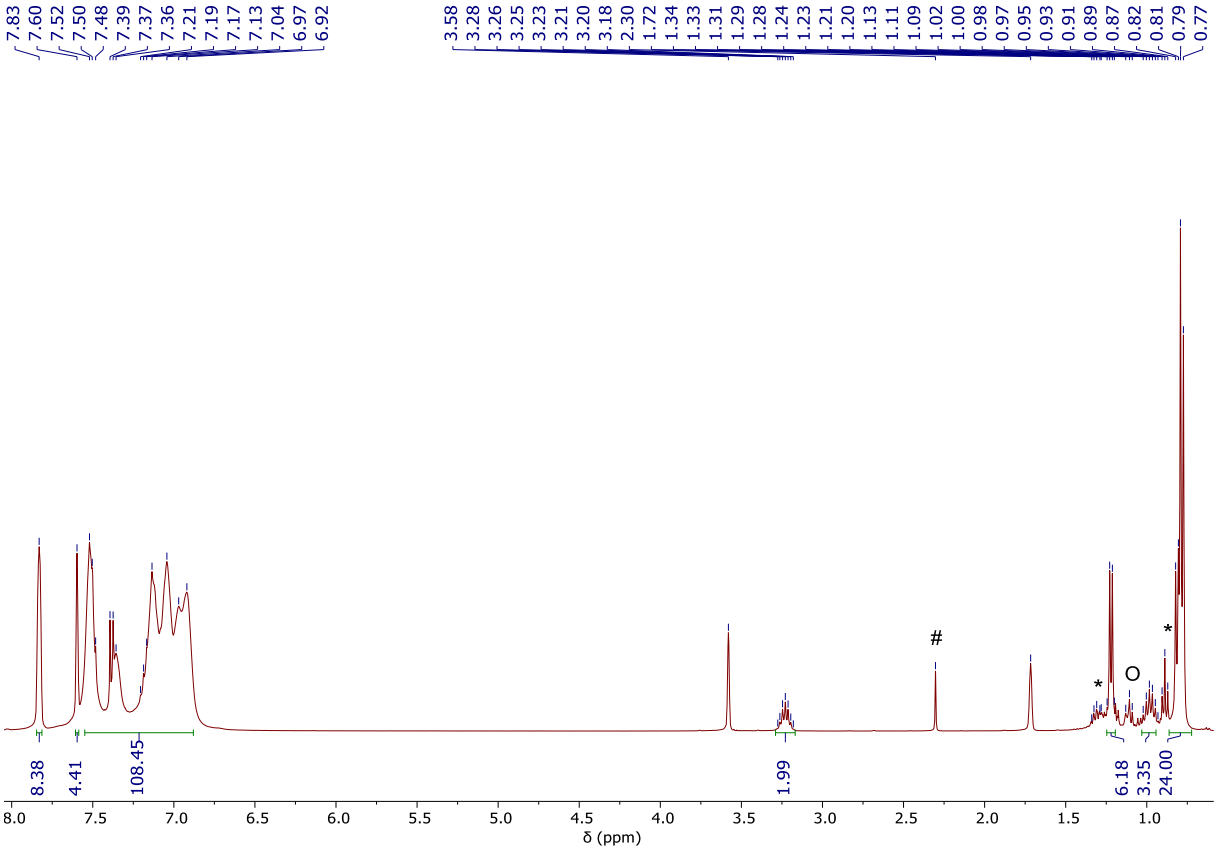

Figure S14. ^{1}H NMR spectrum of **4** with 2 equivs. PPh_3 as a solution in THF-d_8 at ambient temperature; * indicates presence of *n*-pentane; # indicates presence of toluene; o inidactes presence of small amount of decomposition.

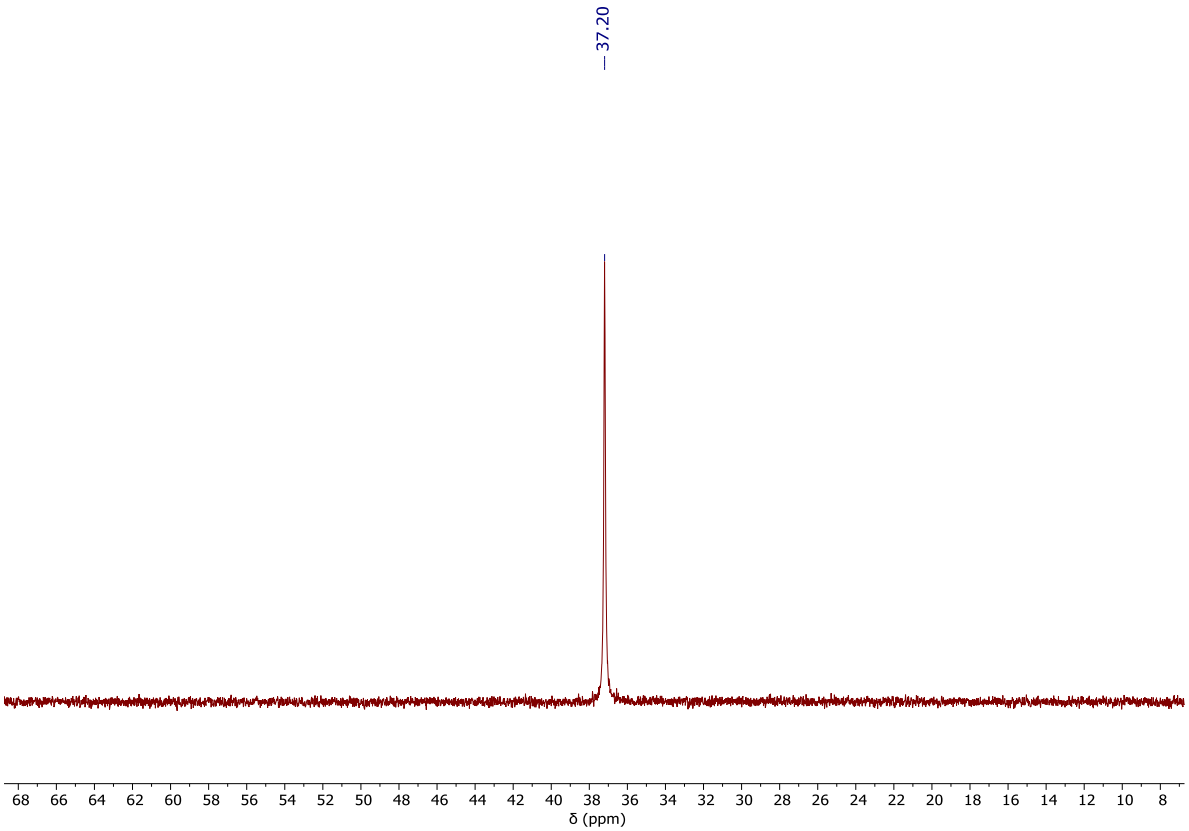

Figure S15. $^{31}P\{^{1}H\}$ NMR spectrum of **4** with 2 equivs. PPh_3 as a solution in THF-d_8 at ambient temperature.

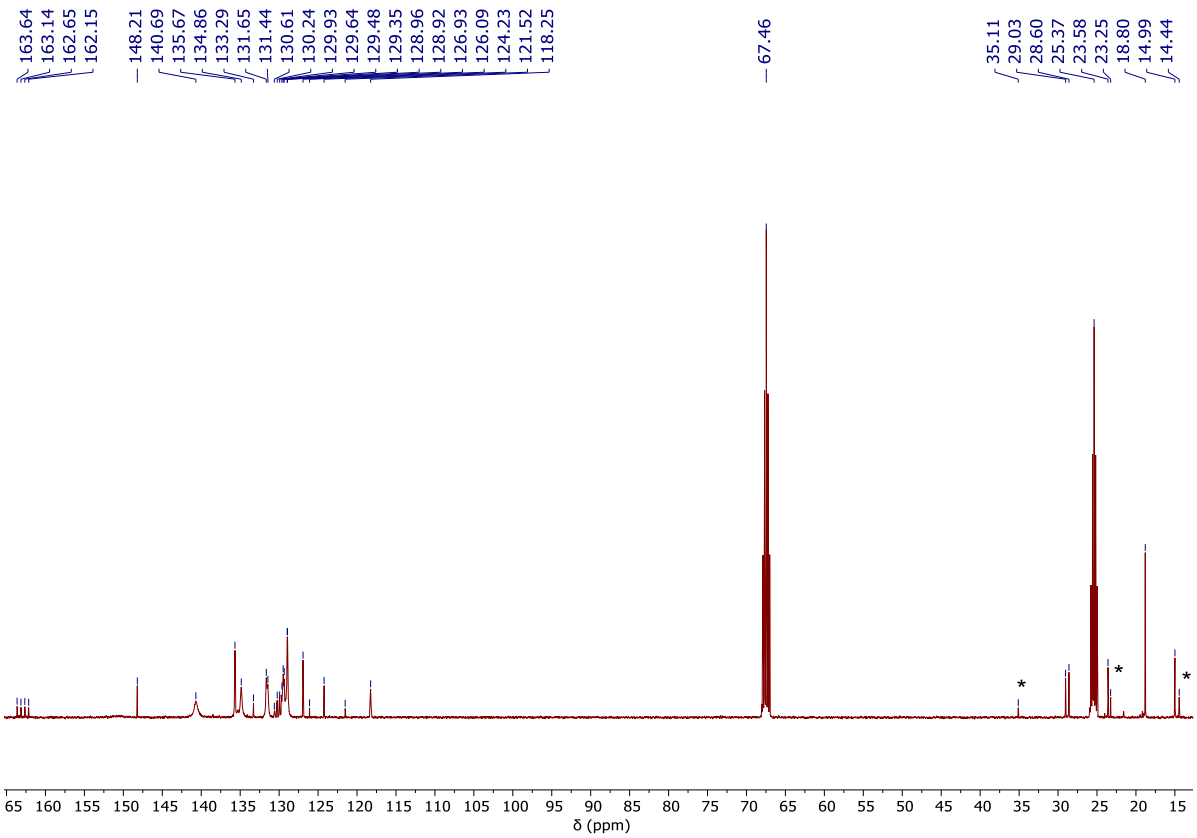

Figure S16. $^{13}C\{^{1}H\}$ NMR spectrum of **4** with 2 equivs. PPh_3 as a solution in THF-d_8 at ambient temperature; * indicates presence of *n*-pentane.

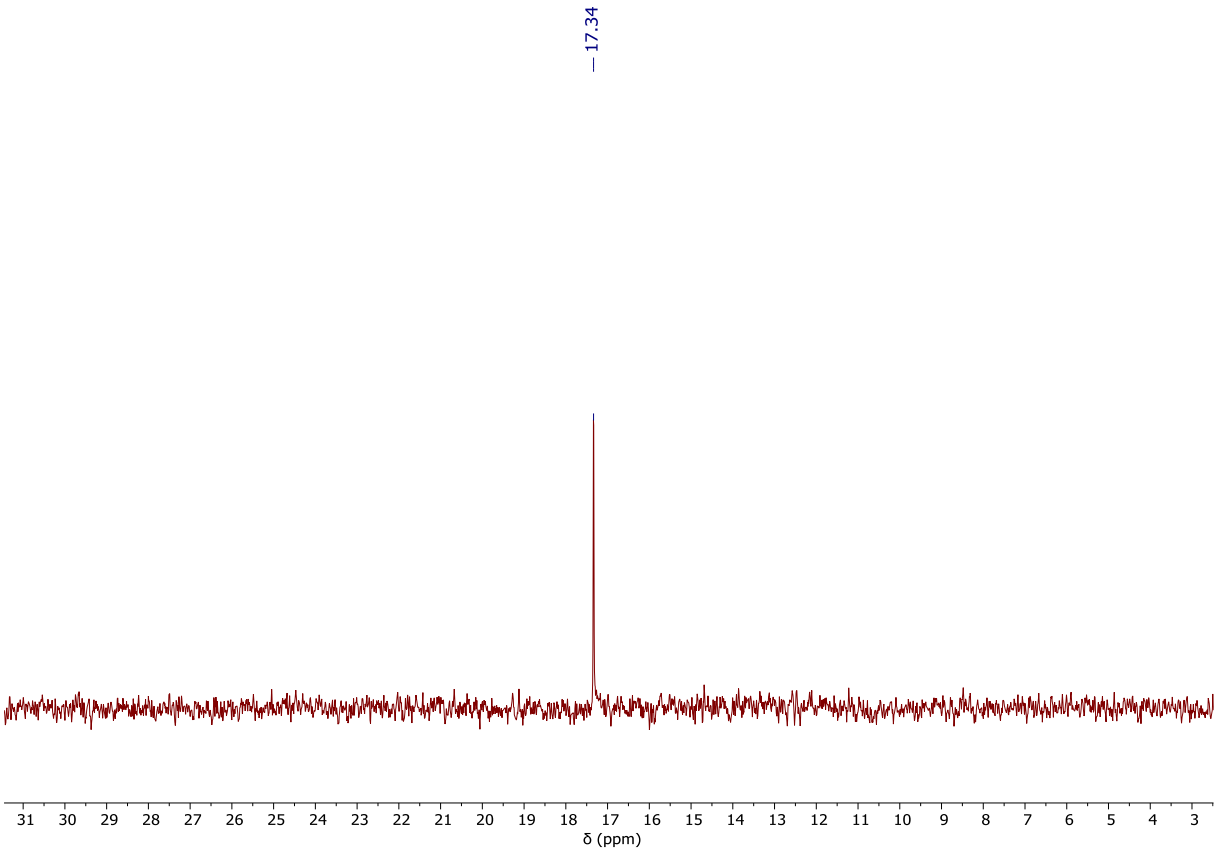

Figure S17. $^{29}Si\{^{1}H\}$ NMR spectrum of **4** with 2 equivs. PPh_3 as a solution in THF-d_8 at ambient temperature.

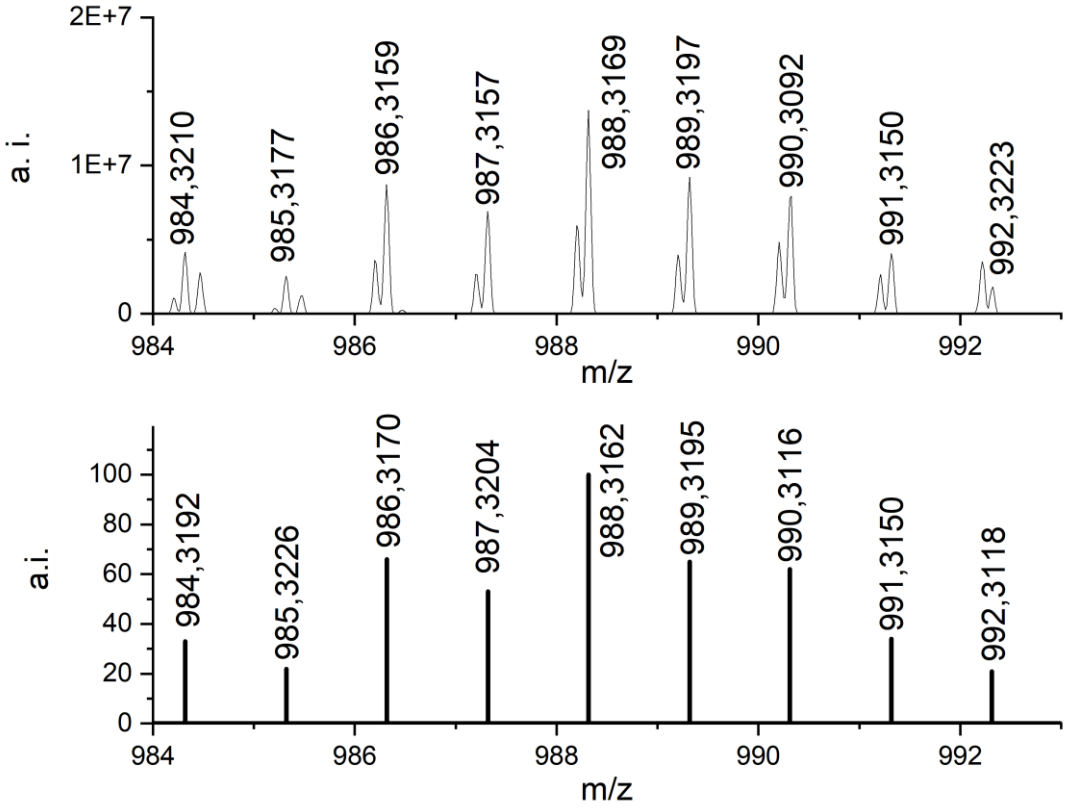

Figure S18. *Top*: Cutout from LIFDI/MS of **4**; *Bottom*: Calculated MS spectrum of **4**.

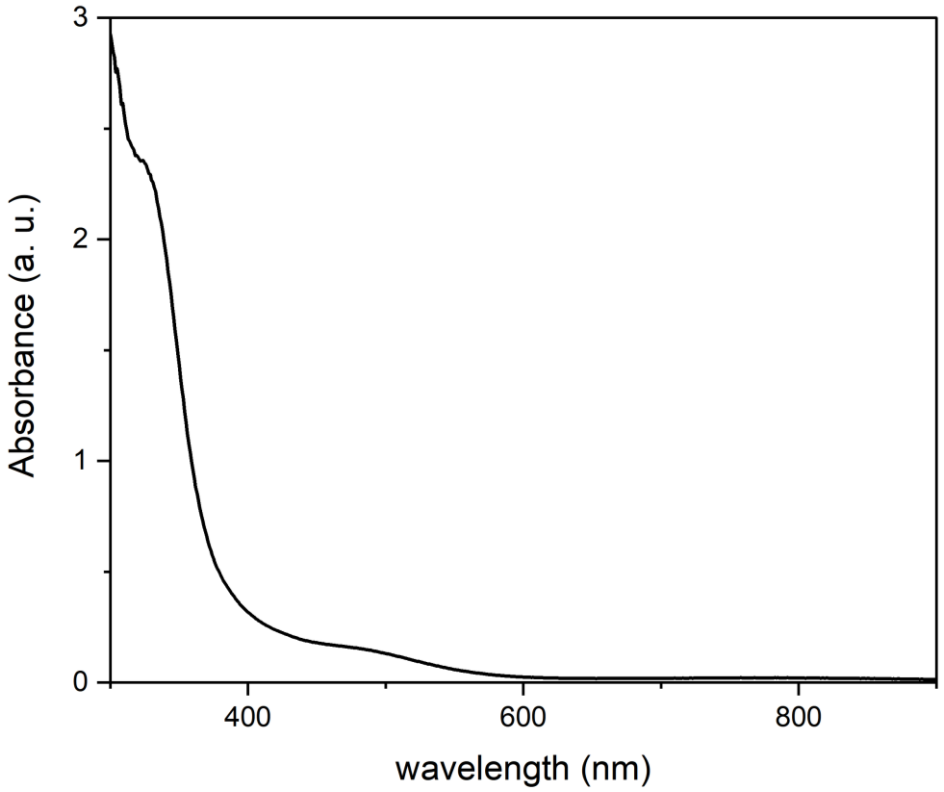

Figure S19. UV/vis spectrum of a 2.5x10^{-4} M solution of **4** in fluorobenzene at ambient temperature.

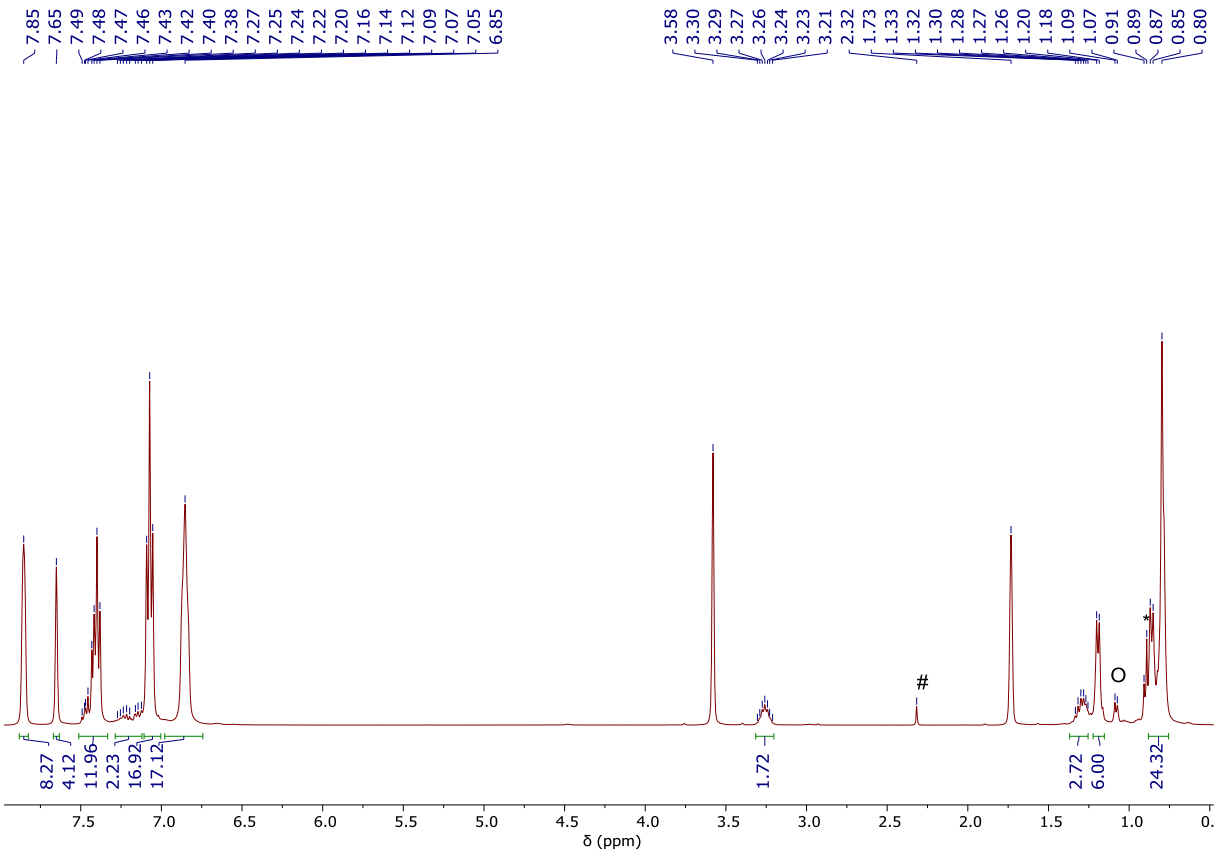

Figure S20. ^{1}H NMR spectrum of **5** as a solution in THF-d_8 at 233 K ; * indicates presence of *n*-pentane; # indicates presence of toluene; o inidactes presence of small amount of decomposition.

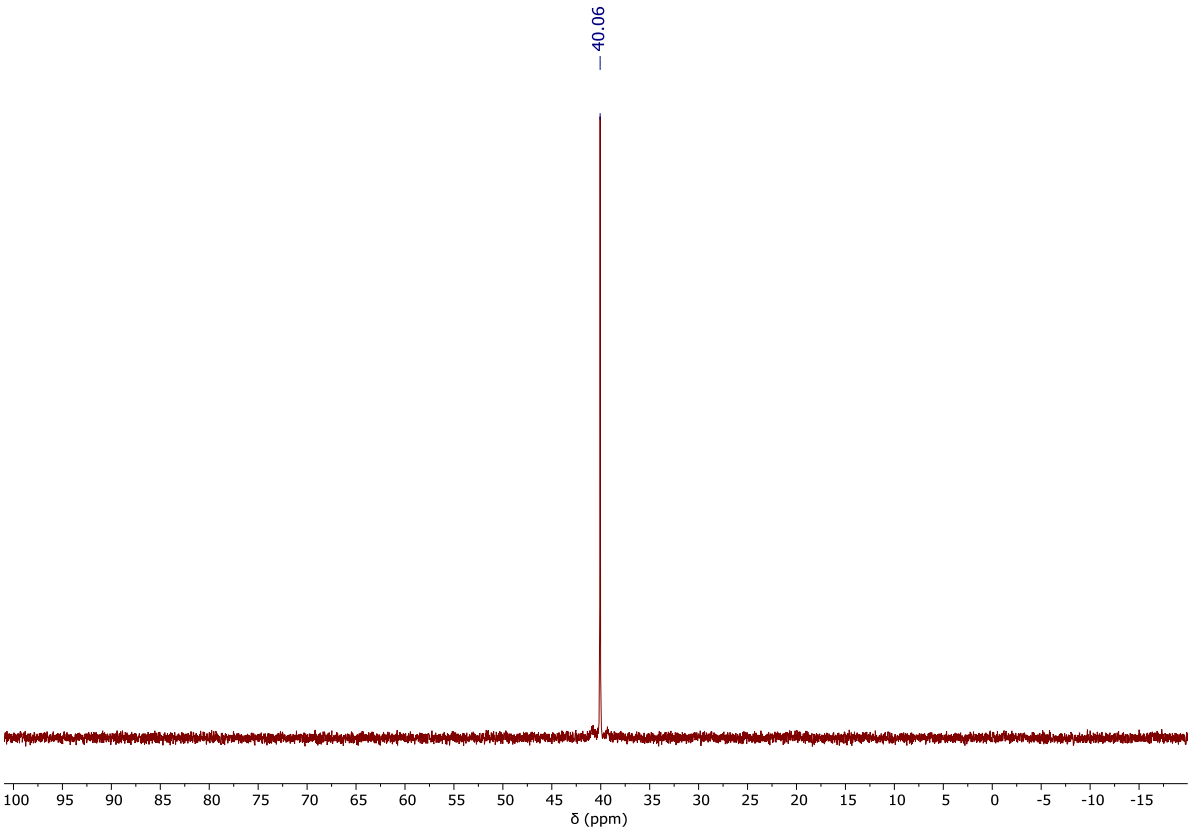

Figure S21. $^{31}P\{^{1}H\}$ NMR spectrum of **5** as a solution in THF-d_8 at 233 K.

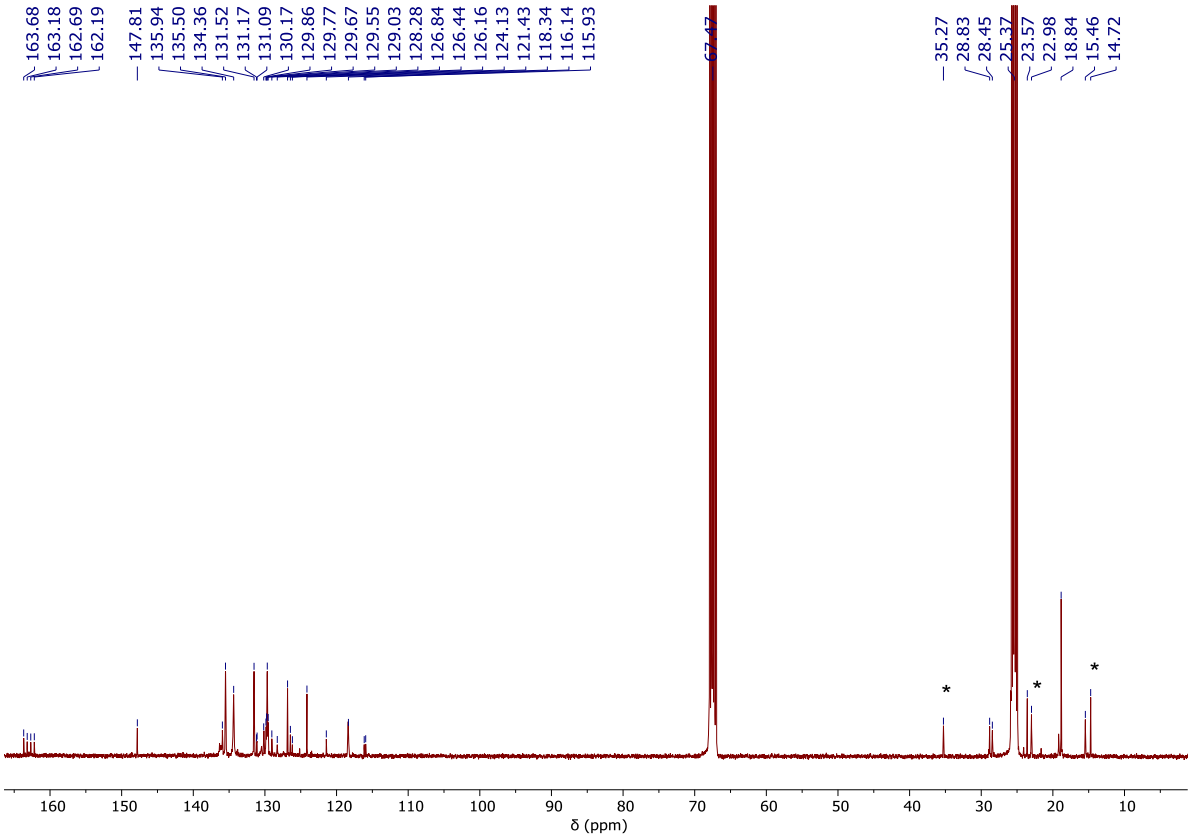

Figure S22. $^{13}C\{^{1}H\}$ NMR spectrum of **5** as a solution in THF-d_8 at 233 K; * indicates presence of *n*-pentane.

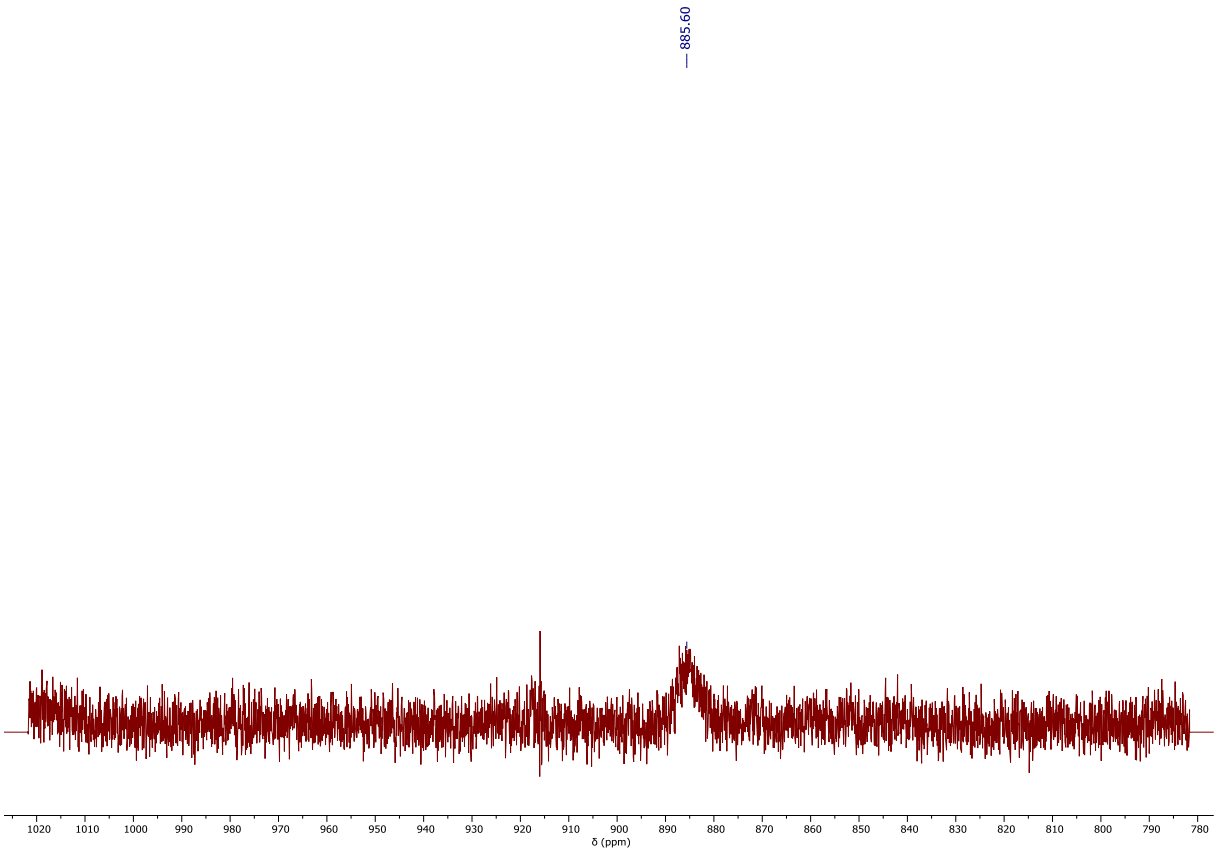

Figure S23. $^{119}Sn\{^{1}H\}$ NMR spectrum of **5** as a solution in THF-d_8 at 233 K.

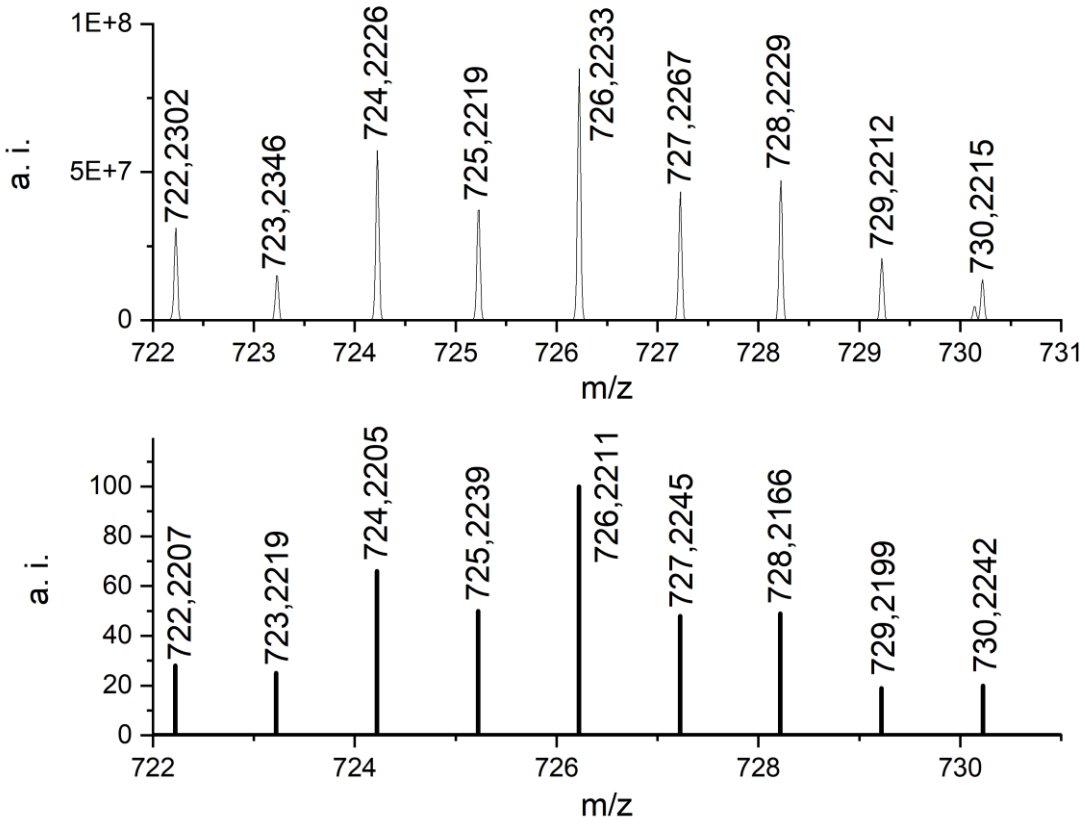

Figure S24. *Top*: Cutout from LIFDI/MS of **5**; *Bottom*: Calculated MS spectrum of **5**.

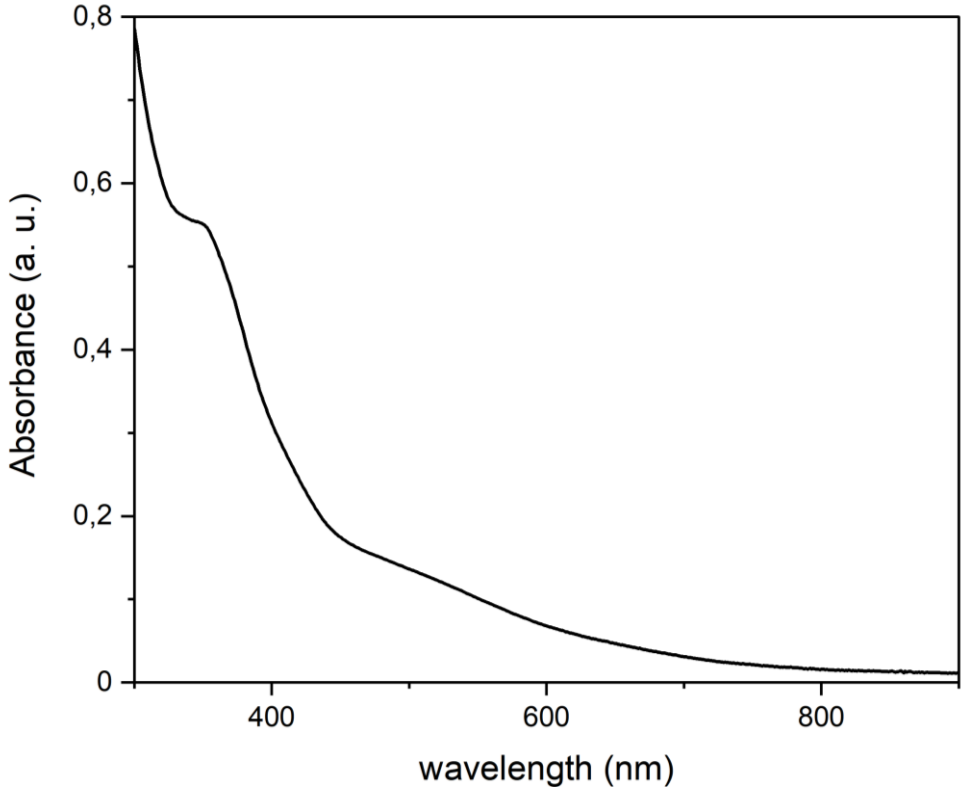

Figure S25. UV/vis spectrum of a 1.0x10^{-4} M solution of **5** in fluorobenzene at ambient temperature.

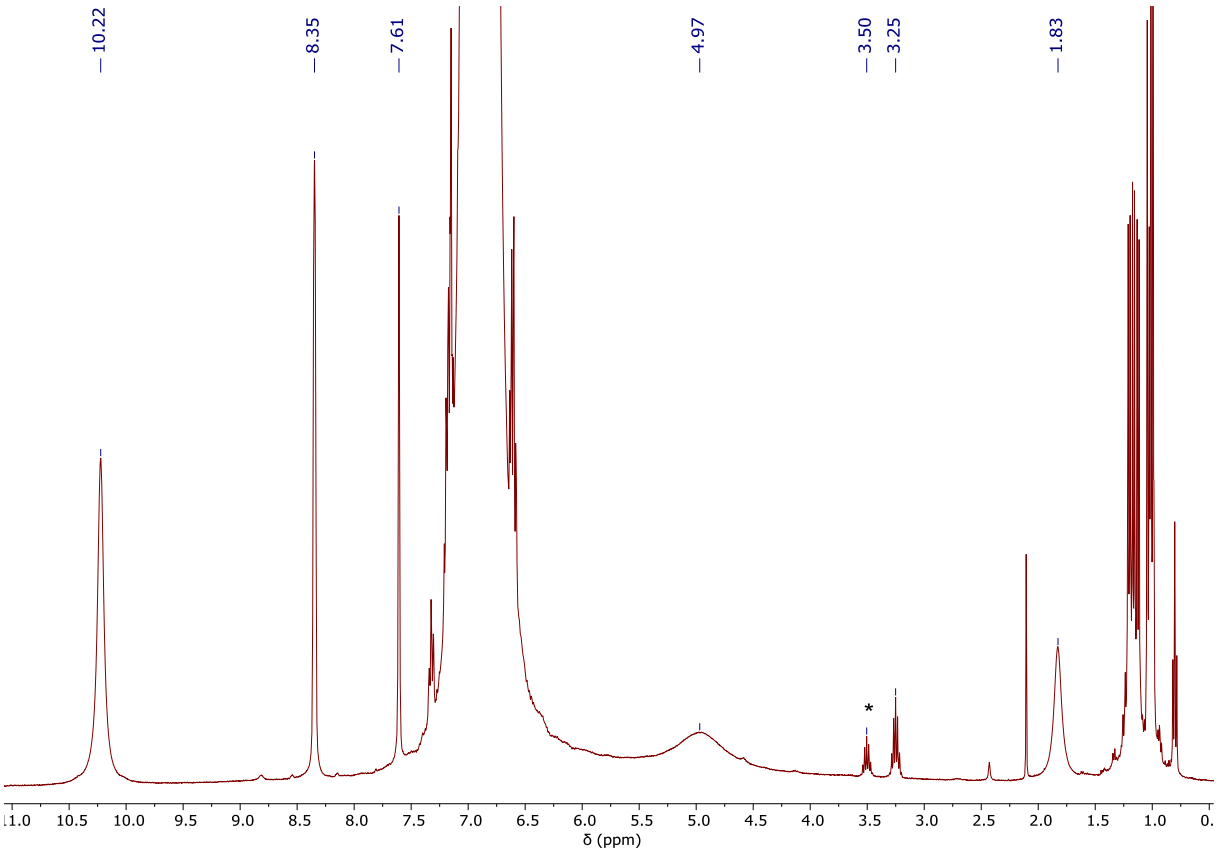

Figure S26. ^{1}H NMR spectrum from the crude reaction mixture of **4** and [PPh_4][SbF_6] in fluorobenzene/C_6D_6 at ambient temperature; * indicates presence of decomposition product ^{SiiP}DippH.

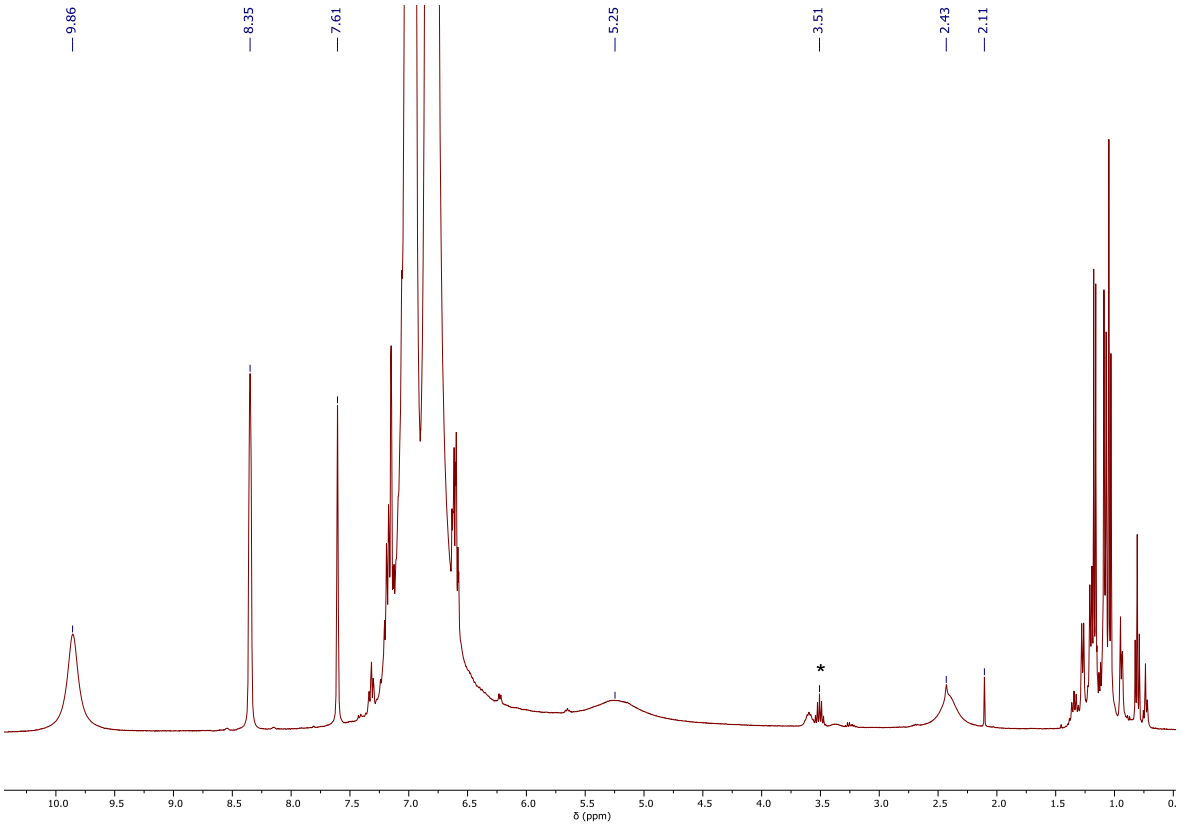

Figure S27. ^{1}H NMR spectrum from the crude reaction mixture of **5** and [PPh_4][SbF_6] in fluorobenzene/C_6D_6 at ambient temperature; * indicates presence of decomposition product ^{SiiP}DippH.

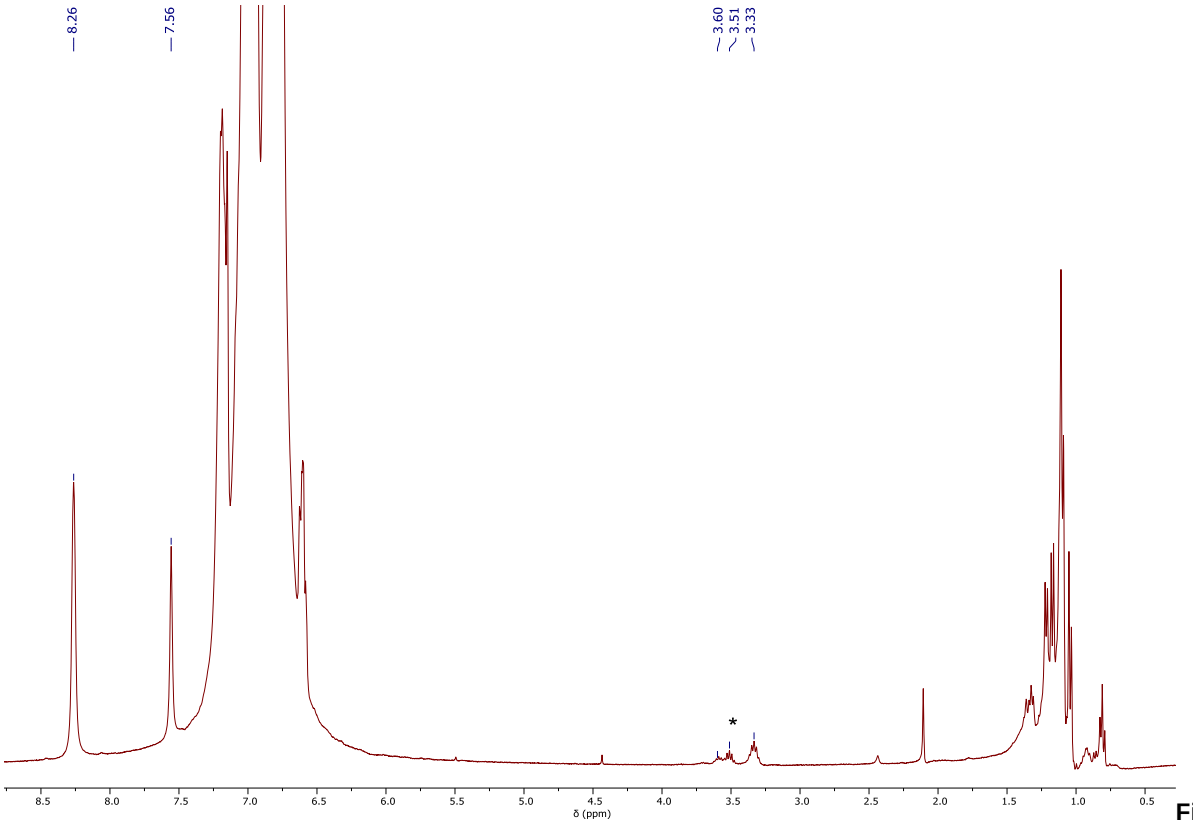

Figure S28. ^{1}H NMR spectrum from the crude reaction mixture of **4** and NH_3 in fluorobenzene/C_6D_6 at ambient temperature; * indicates presence of decomposition product ^{SiiP}DippH.

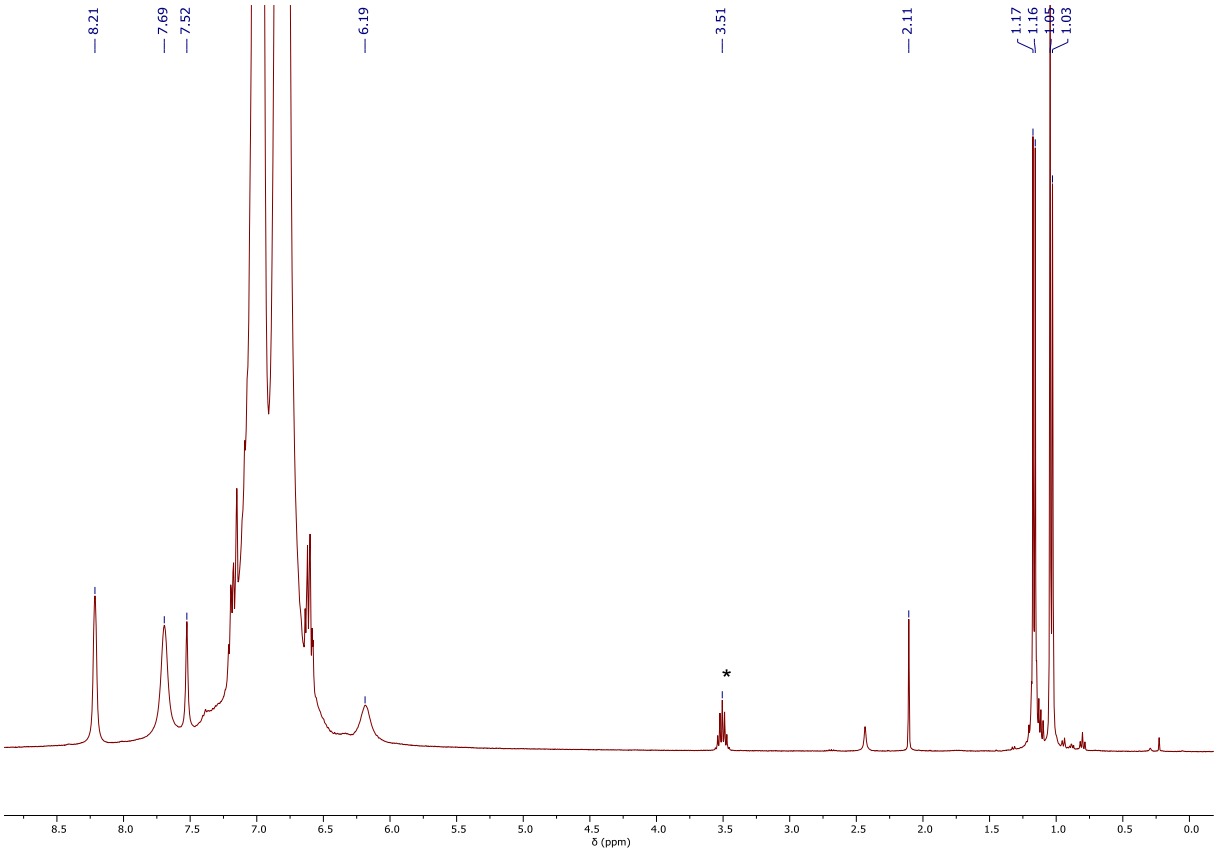

Figure S29. ^{1}H NMR spectrum from the crude reaction mixture of **5** and NH_3 in fluorobenzene/C_6D_6 at ambient temperature; *indicates presence of decomposition product ^{SiiP}DippH.

2. X-ray crystallographic details

Single crystals of **1**, **2**, **2·KCl**, **3**, **4**, and **5** suitable for X-ray structural analysis were mounted in perfluoroalkyl ether oil on a nylon loop and positioned in a 150 K cold N_2 gas stream. Data collection was performed with a STOE StadiVari diffractometer (MoKα radiation) equipped with a DECTRIS PILATUS 300K detector. Structures were solved by Direct Methods (SHELXS-97)[5] and refined by full-matrix least-squares calculations against F^2 (SHELXL-2018).[6] The positions of the hydrogen atoms were calculated and refined using a riding model. All non-hydrogen atoms were treated with anisotropic displacement parameters. Crystal data, details of data collections, and refinements for all structures can be found in their CIF files, which are available free of charge via www.ccdc.cam.ac.uk/data_request/cif, and are summarized in Table S1. Details for **3** are not given due to the unpublishable quality of the collected X-ray data. The structure for this compound is given in Figure S33, as proof of connectivity.

Table S1. Summary of X-ray crystallographic data for **1**, **2**, **2·KCl**, **4**, and **5**.

	1	**2**	**2·KCl**	**4·0.55(C_6H_5F), 0.45(C_5H_{12})**	**5·C_6H_6**
empirical form.	$C_{21}H_{38}ClGeNSi$	$C_{42}H_{76}Cl_2N_2Si_2Sn_2$	$C_{42}H_{76}Cl_3KN_2Si_2Sn_2$	$C_{112.5}H_{103.2}BF_{24.6}GeNNiP_3Si$	$C_{113}H_{101}BF_{24}NNiP_3SiSn$
formula wt	440.65	973.50	1048.05	2199.14	2238.15
crystal syst.	monoclinic	triclinic	triclinic	triclinic	triclinic
space group	*P2₁/n*	*P-1*	*P-1*	*P-1*	*P-1*
a (Å)	15.832(3)	9.148(2)	11.130(2)	13.186(3)	13.245(3)
b (Å)	9.619(2)	9.655(2)	14.968(3)	18.874(5)	18.891(4)
c (Å)	16.603(3)	15.011(3)	16.561(3)	22.343(6)	22.423(5)
α (deg.)	90	101.80(3)	72.19(3)	94.774(10)	94.60(3)
β (δεγ)	112.86(3)	96.15(3)	77.40(3)	103.543(11)	103.40(3)
γ (deg.)	90	109.26(3)	79.94(3)	92.404(12)	91.59(3)
vol (Å^3)	2329.9(9)	1203.1(5)	2546.1(10)	5376(2)	5434.2(2)
Z	4	1	2	2	2
ρ(calc) (g.cm^{-3})	1.257	1.343	1.367	1.359	1.368
μ (mm^{-1})	1.486	1.227	1.296	0.600	0.546
F(000)	936	504	1080	2261	2288
T (K)	150(2)	150(2)	150(2)	150(2)	150(2)
reflns collect.	13412	16820	27458	48303	71208
unique reflns	4014	4727	9943	21106	21204
R_{int}	0.0907	0.0131	0.0438	0.0346	0.1473
R1 [$I>2\sigma(I)$]	0.0519	0.0167	0.0347	0.0590	0.0957
*w*R2 (all data)	0.1094	0.0439	0.0631	0.1733	0.2688
CCDC No.	2143456	2143457	2143458	2143459	2143460

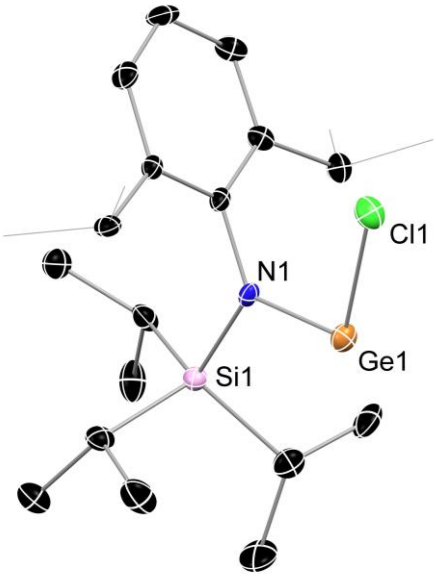

Figure S30. Molecular structure of ^{SiiP}DippGeCl, with thermal ellipsoids at 30% probability, hydrogen atoms omitted, and peripheral substituents in wire-frame for clarity. Selected bond lengths (Å) and angles (°): Ge1-N1 1.843(5); Ge1-Cl1 2.226(1); N1-Ge1-Cl1 100.1(1).

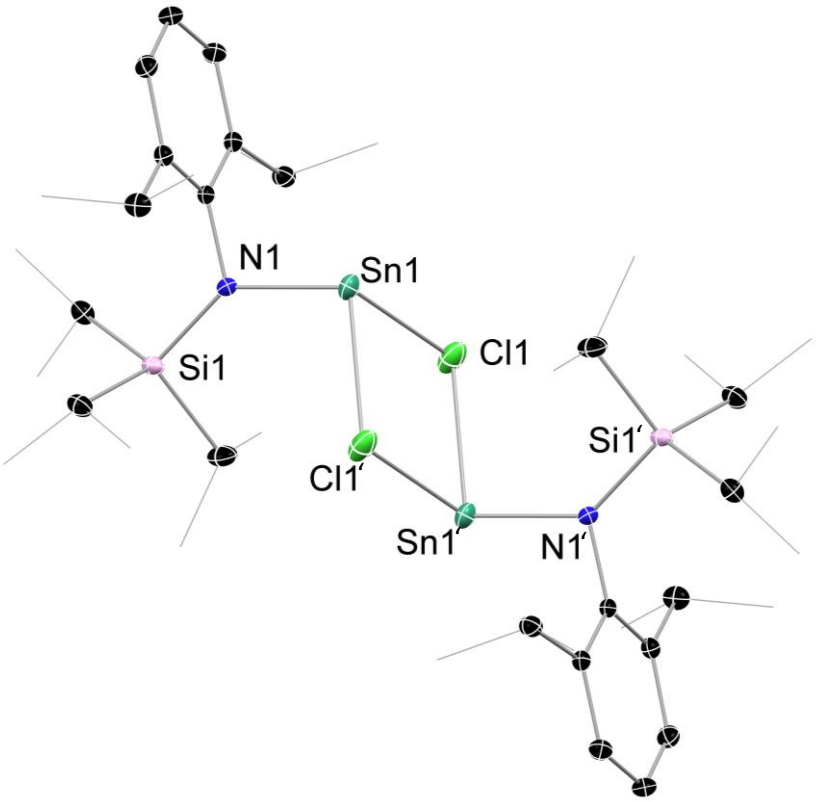

Figure S31. Molecular structure of [^{SiiP}DippSnCl]$_2$, with thermal ellipsoids at 30% probability, hydrogen atoms omitted, and peripheral substituents in wire-frame for clarity. The prime label (') indicates atoms at the equivalent position, (2-x, 1-y, 2-z). Selected bond lengths (Å) and angles (°): Sn1-N1 2.083(1); Sn1-Cl1 2.620(1); Sn1-Cl1' 2.7290(9); Sn1···Sn1' 4.081(2); N1-Sn1-Cl1 102.88(4); N1-Sn1-Cl1' 103.19(4); N1-Sn1-Sn1' 107.20(3).

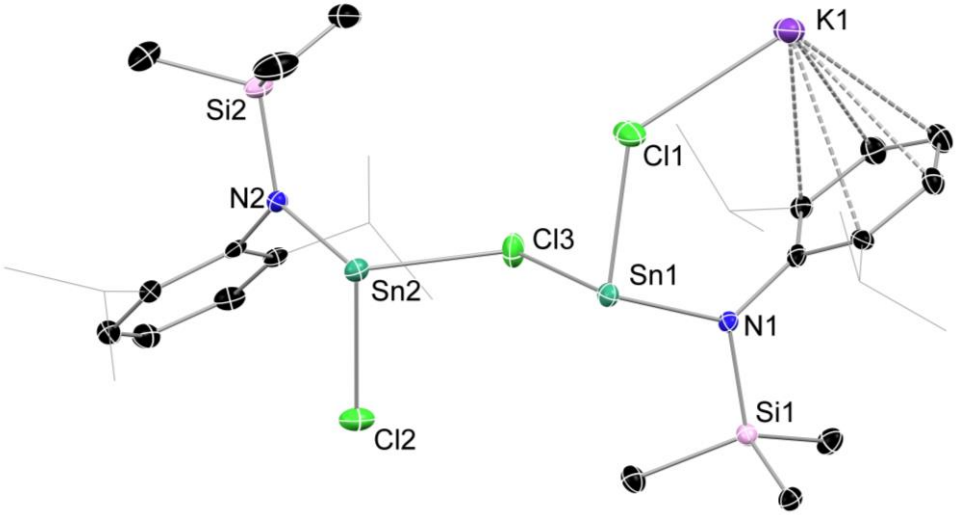

Figure S32. Molecular structure of [^{SiiP}DippSnCl]$_2$·KCl, with thermal ellipsoids at 30% probability, hydrogen atoms omitted, and peripheral substituents in wire-frame for clarity. Selected bond lengths (Å) and angles (°): N1-Sn1 2.116(3); Cl1-Sn1 2.470(1); Cl3-Sn1 2.664(1); N2-Sn2 2.125(3); Cl2-Sn2 2.475(1); Cl3-Sn2 2.631(1); Cl1-K1 2.948(2); Sn1···Sn2 3.929(1); Sn1-Cl3-Sn2 95.81(4) N1-Sn-Cl1 98.75(8); N1-Sn1-Cl3 96.22(8); N2-Sn2-Cl2 98.66(8); N2-Sn2-Cl3 98.91(8); Sn1-Cl3-Sn2 95.81(4).

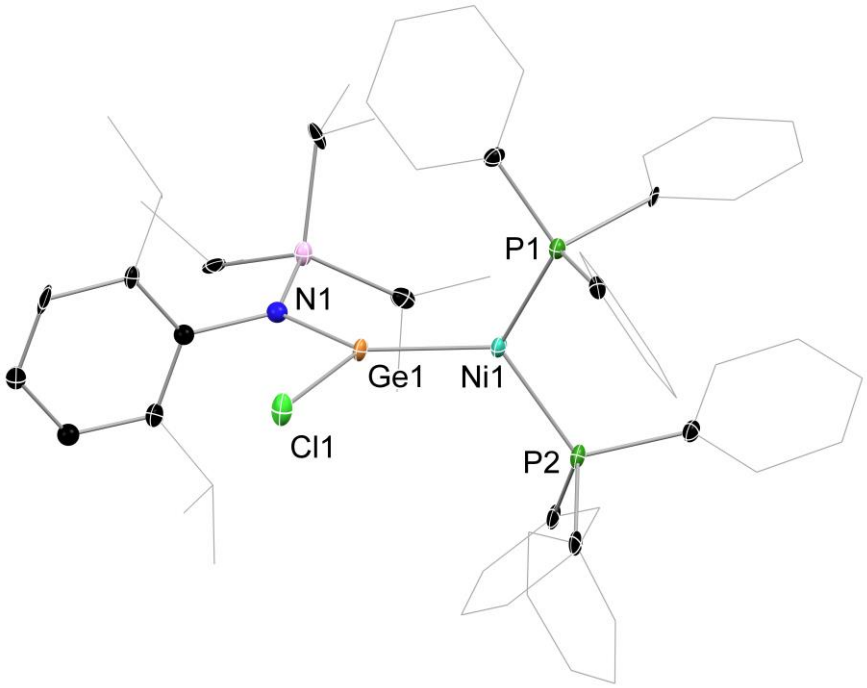

Figure S33. Molecular structure of [^{SiiP}DippSnCl]$_2$·KCl, with thermal ellipsoids at 30% probability, hydrogen atoms omitted, and peripheral substituents in wire-frame for clarity. Metrical parameters are not discussed due to the low quality of the collected data.

3. Computational methods and details

Computational experiments were performed using the Gaussian 16 program.[7] Geometry optimization was carried out at the ωB97XD level with the def2-TZVPP basis set for Ni, Ge, and Sn, and the def2-SVP basis set for all other atoms.[8] Stationary points were confirmed as true minima by vibrational frequency analysis (no negative eigenvalues). Bond indices (Wiberg Bond Index, Mayer Bond Order) and NPA charges were determined using the NBO 6.0 program implemented in Gaussian 09, using optimized geometries from above.[9] Dative interactions were determined through the NBO-derived second order perturbation theory analysis, and visualized in ChemCraft through combination of the associated MOs.

Table S2. Summary of NBO parameters for donor-acceptor orbitals in **4**.

		Orbital number	Occupancy	Composition (%)		
				s	*p*	*d*
Lone pairs	**Ge**	120	1.824	92.11	0.09	0.00
	Ni	121	1.970	0.00	0.02	99.98
	Ni	122	1.969	0.00	0.01	99.98
	Ni	123	1.966	0.04	0.02	99.93
	Ni	124	1.850	0.01	0.02	99.97
	Ni	125	1.766	0.00	0.02	99.98
Vacant orbitals	**Ge**	330	0.431	0.00	99.83	0.05
	Ge	331	0.400	0.17	99.53	0.22
	Ni	333	0.395	99.89	0.04	0.06

Table S3. Summary of NBO parameters for donor-acceptor orbitals in **5**.

		Orbital number	Occupancy	Composition (%)		
				s	*p*	*d*
Lone pairs	**Sn**	115	1.779	98.33	1.63	0.03
	Ni	116	1.973	0.21	0.11	99.68
	Ni	117	1.967	0.00	0.01	99.99
	Ni	118	1.964	0.01	0.02	99.97
	Ni	119	1.897	0.03	0.08	99.89
	Ni	120	1.843	0.09	0.17	99.75
Vacant orbitals	**Sn**	325	0.270	0.01	99.79	0.00
	Sn	326	0.251	0.02	99.73	0.18
	Ni	328	0.474	98.53	1.03	0.44

NBO visualization of major contributions to the Ge-Ni donor-acceptor bonds in **4**:

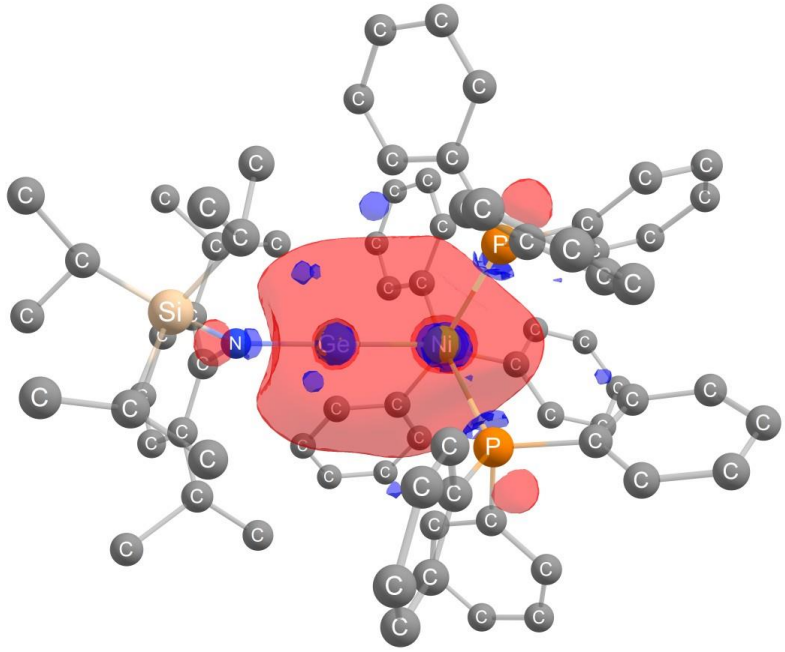

Figure S34. Ge→Ni donor interaction (MO120 to MO333, 92.40 kcalmol^{-1}).

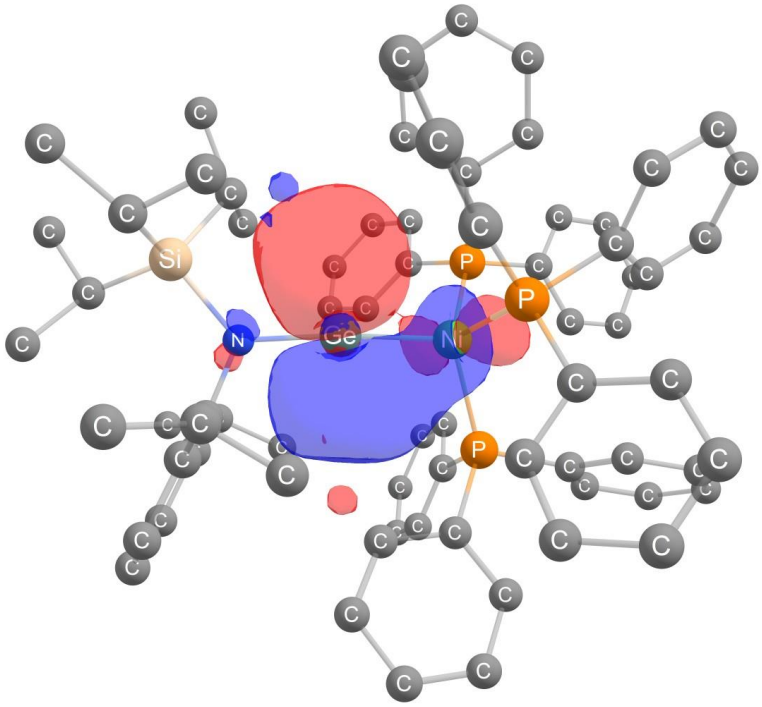

Figure S35. Ge→Ni donor interaction (MO124 to MO330, 18.98 kcalmol^{-1}).

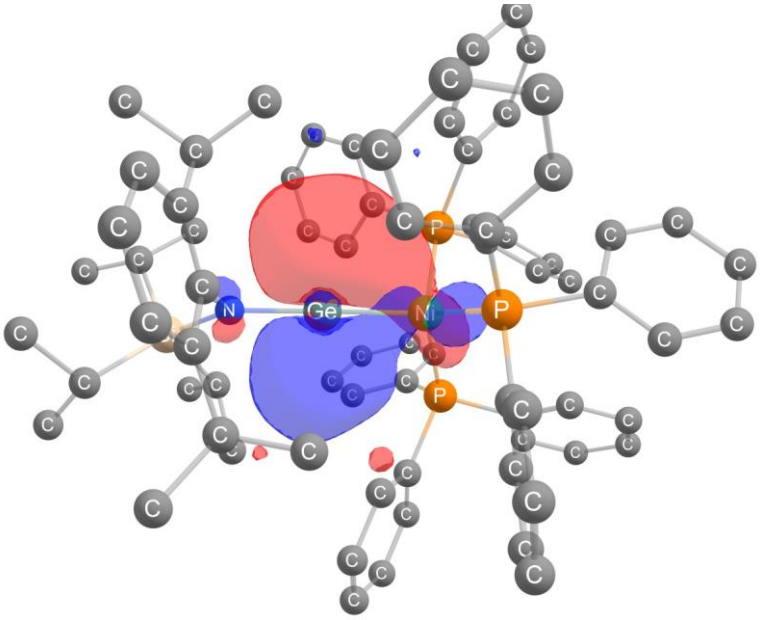

Figure S36. Ge→Ni donor interaction (MO125 to MO331, 28.00 kcalmol^{-1}).

NBO visualization of major contributions to the Sn-Ni donor-acceptor bonds in **5**:

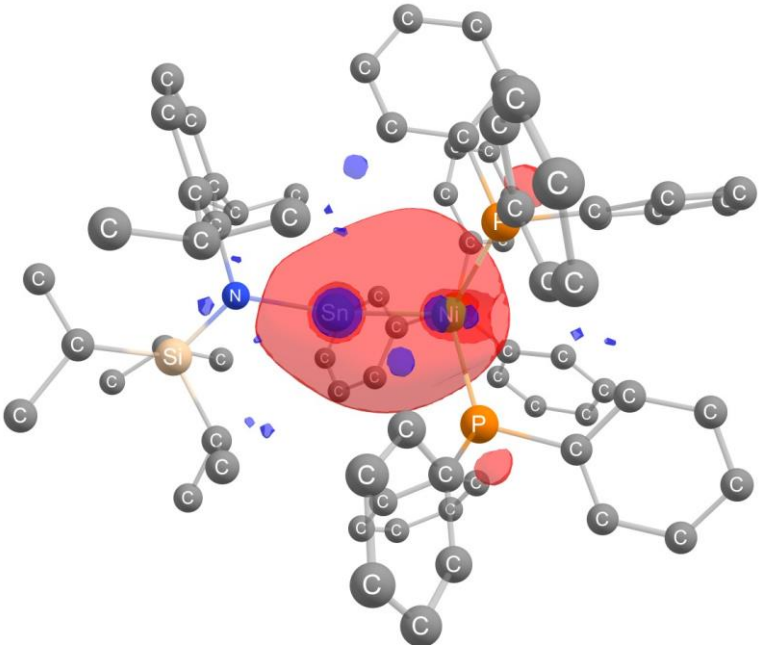

Figure S37. Ge→Ni donor interaction (MO115 to MO328, 141.27 kcalmol^{-1}).

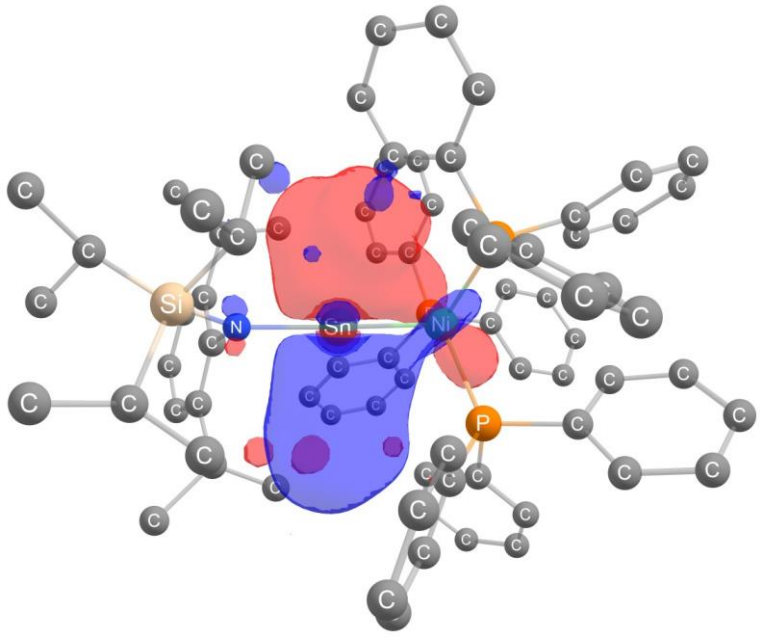

Figure S38. Ge→Ni donor interaction (MO119 to MO325, 6.24 kcalmol^{-1}).

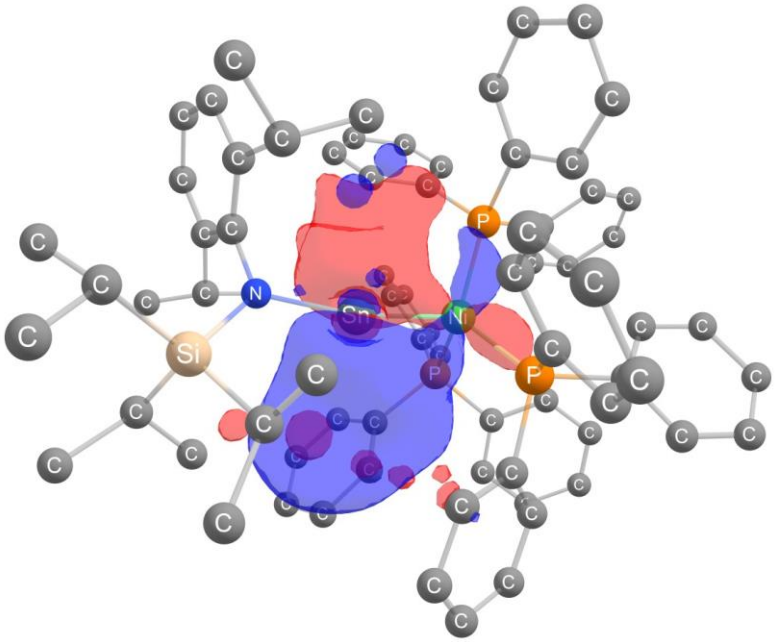

Figure S39. Ge→Ni donor interaction (MO120 to MO326, 10.80 kcalmol^{-1}).

Table S4. Cartesian geometry of **4**.

Atom	x-Coordinate	y-Coordinate	z- Coordinate
Ge	-1.28945	-0.02892	0.01493
Ni	0.83644	0.037	0.0513
P	1.60351	2.16717	0.5152
P	1.50883	-1.57561	1.56083
P	1.48993	-0.65709	-2.04851
Si	-4.31151	-1.24734	0.22899

N	-3.09555	0.09418	-0.00719
C	-3.79196	2.28043	0.93135
C	3.41592	2.45103	0.27532
C	3.26707	-1.63211	2.12279
C	1.2041	1.81498	-3.32039
H	0.43763	1.99523	-2.56949
C	-0.08956	-2.93246	-2.38392
H	0.24279	-3.18274	-1.37647
C	1.68152	4.55969	-1.02723
H	2.76151	4.55476	-0.87639
C	5.3804	-3.1849	-1.8957
H	6.29718	-3.77471	-1.83212
C	3.98999	2.11339	-0.95701
H	3.36954	1.71775	-1.75982
C	-3.58909	1.44395	-0.19372
C	2.93007	0.41802	-4.25815
H	3.50592	-0.50926	-4.26542
C	-0.13777	-1.42217	-4.26506
H	0.16456	-0.49121	-4.74817
C	2.22479	-3.96627	0.21856
H	3.20453	-3.5135	0.06382
C	4.04964	-0.48105	2.01254
H	3.63211	0.4182	1.566
C	1.3764	2.81601	2.22707
C	0.88653	3.54006	-0.49033
C	1.48355	2.80529	-4.25944
H	0.91718	3.7385	-4.24039
C	0.31106	-1.72624	-2.97572
C	5.37654	-0.46394	2.43754
H	5.96116	0.45217	2.32962
C	1.60078	2.46193	4.61997
H	1.87878	1.80767	5.44862
C	3.17764	-2.83418	-2.83611
H	2.38206	-3.15984	-3.50864
C	1.91751	0.61369	-3.30903
C	4.05157	-1.29951	-1.19557
H	3.93765	-0.41325	-0.57292
C	0.90458	4.10946	2.48259
H	0.63077	4.7692	1.65807
C	1.96483	-5.21978	-0.33308
H	2.74399	-5.71936	-0.91192
C	-4.34773	3.54678	0.73111

H	-4.51279	4.19982	1.58992
C	-1.31255	-3.53444	-4.37622
H	-1.93474	-4.24256	-4.92733
C	5.2287	-2.03849	-1.11608
H	6.01663	-1.72296	-0.42873
C	4.35675	-3.57466	-2.75982
H	4.47382	-4.46668	-3.37896
C	1.11253	3.74444	4.86437
H	1.00535	4.10548	5.88931
C	-3.90536	1.90629	-1.49404
C	1.73024	2.00408	3.31141
H	2.1188	0.99963	3.1436
C	-4.46946	3.17683	-1.63594
H	-4.72903	3.53737	-2.63318
C	-0.95765	-2.31798	-4.95411
H	-1.30147	-2.06814	-5.96005
C	5.94378	-1.61393	2.98036
H	6.98457	-1.61181	3.31075
C	1.24265	-3.29789	0.96027
C	3.21717	1.41121	-5.19238
H	4.01196	1.25027	-5.92368
C	-2.03393	2.53372	2.68031
H	-1.24696	2.22642	1.9773
H	-1.69318	2.27169	3.69357
H	-2.09785	3.63109	2.62333
C	-3.37869	1.88552	2.34204
H	-3.23775	0.79677	2.35927
C	3.01123	-1.69263	-2.0434
C	2.49507	2.60536	-5.19639
H	2.72636	3.3815	-5.92885
C	0.76925	4.56646	3.79244
H	0.39373	5.57558	3.97404
C	-0.25678	-5.17461	0.59597
H	-1.22923	-5.64428	0.75664
C	-0.7207	-1.53238	5.64954
H	-1.23448	-1.51227	6.61279
C	-0.82169	-0.45302	4.77843
H	-1.41597	0.42157	5.05146
C	0.60327	-1.58846	3.17277
C	-0.17233	-0.48879	3.5444
H	-0.27033	0.35819	2.86519
C	-4.42621	2.22669	3.40614

H	-4.49929	3.31115	3.57831
H	-4.1506	1.76581	4.36668
H	-5.42699	1.86468	3.12855
C	3.84808	-2.7825	2.67528
H	3.27485	-3.70723	2.76014
C	-0.87519	-3.83937	-3.08722
H	-1.15068	-4.78603	-2.61772
C	0.00404	-3.92369	1.15077
H	-0.76381	-3.43501	1.75042
C	1.10552	5.59367	-1.76476
H	1.74326	6.37631	-2.18075
C	5.17482	-2.77265	3.09742
H	5.61265	-3.67957	3.51928
C	0.04025	-2.64554	5.28484
H	0.12091	-3.49922	5.96064
C	0.70248	-2.66961	4.06201
H	1.28769	-3.55096	3.79415
C	0.72314	-5.82542	-0.15337
H	0.52198	-6.80698	-0.5873
C	-0.27187	5.62978	-1.96941
H	-0.72103	6.4401	-2.54736
C	-6.71408	0.33685	0.42057
H	-7.22448	-0.22337	-0.37862
H	-6.19594	1.18481	-0.04791
H	-7.49958	0.75165	1.07298
C	4.23684	2.99565	1.27112
H	3.81935	3.28518	2.23607
C	-0.49692	3.59273	-0.69569
H	-1.14975	2.82095	-0.28416
C	5.35175	2.29097	-1.18419
H	5.77383	2.01692	-2.15313
C	-4.7495	1.0932	-3.75963
H	-4.85973	2.06856	-4.25791
H	-5.71403	0.84752	-3.28999
H	-4.55256	0.34864	-4.54563
C	6.16544	2.81258	-0.17946
H	7.23478	2.94946	-0.35289
C	-3.6082	1.0907	-2.74049
H	-3.45415	0.05543	-2.42637
C	-1.07503	4.6275	-1.42588
H	-2.15681	4.64021	-1.56611
C	-5.77366	-0.56967	1.23033

H	-5.31504	0.04399	2.02238
C	-3.02342	-2.13365	2.61306
H	-3.93928	-2.1554	3.22218
H	-2.61068	-1.11875	2.68554
H	-2.29849	-2.80461	3.10431
C	-2.29238	1.54779	-3.37199
H	-2.04843	0.94195	-4.25755
H	-1.46251	1.43966	-2.65925
H	-2.32937	2.60673	-3.67328
C	-3.30459	-2.55597	1.167
H	-2.33792	-2.57963	0.62088
C	5.60241	3.16912	1.04441
H	6.22764	3.59283	1.8332
C	-3.73654	-2.49186	-2.26641
H	-3.43265	-3.46252	-1.84618
H	-2.8312	-1.86405	-2.29351
H	-4.029	-2.67227	-3.31326
C	-4.70281	3.99132	-0.5355
H	-5.15056	4.97848	-0.66575
C	-6.09279	-2.81889	-1.42371
H	-6.35938	-3.13802	-2.44431
H	-6.98302	-2.33976	-0.99323
H	-5.89266	-3.7314	-0.84241
C	-4.88387	-1.87218	-1.46609
H	-5.219	-0.96213	-1.9918
C	-6.57542	-1.67617	1.93611
H	-7.38791	-1.23218	2.53353
H	-5.95944	-2.27409	2.62253
H	-7.04431	-2.37068	1.22321
C	-3.8596	-3.98436	1.11662
H	-3.2216	-4.66337	1.70652
H	-3.90559	-4.3805	0.09257
H	-4.87173	-4.04775	1.54431

Table S5. Cartesian geometry of **5**.

Atom	**x-Coordinate**	**y-Coordinate**	**z- Coordinate**
Sn	-1.24859	-0.13188	-0.0352
Ni	1.07134	0.04305	0.061
P	1.66086	2.15407	0.65251
P	1.65158	-1.64299	1.48655

P	1.65292	-0.51999	-2.07633
Si	-4.44479	-1.26176	0.18257
N	-3.26305	0.07856	-0.01443
C	-3.87414	2.25039	0.9981
C	3.47221	2.47707	0.4749
C	3.41296	-1.75675	2.02031
C	1.27712	1.98285	-3.24635
H	0.45503	2.07331	-2.53724
C	-0.03933	-2.69939	-2.50433
H	0.28183	-3.00548	-1.50843
C	1.71502	4.59859	-0.80837
H	2.79327	4.60656	-0.64439
C	5.47375	-3.14921	-2.08168
H	6.37136	-3.77021	-2.04904
C	4.0797	2.1949	-0.75566
H	3.47958	1.8363	-1.59102
C	-3.7045	1.43973	-0.15327
C	3.14331	0.74882	-4.14801
H	3.77698	-0.13997	-4.16734
C	0.01386	-1.13258	-4.33811
H	0.37474	-0.20882	-4.79365
C	2.26505	-3.97465	-0.00874
H	3.2598	-3.55045	-0.15176
C	4.19048	-0.5958	1.99684
H	3.76246	0.33776	1.63643
C	1.36993	2.7093	2.38601
C	0.93244	3.55125	-0.30967
C	1.53989	3.03393	-4.12113
H	0.91038	3.92547	-4.09428
C	0.43758	-1.5014	-3.05717
C	5.52465	-0.61274	2.39792
H	6.10632	0.31085	2.36129
C	1.56671	2.237	4.76068
H	1.86014	1.5535	5.55991
C	3.28522	-2.68022	-3.00307
H	2.48052	-2.9444	-3.69176
C	2.07075	0.83131	-3.25098
C	4.20372	-1.26292	-1.28082
H	4.11498	-0.40777	-0.61079
C	0.83237	3.96346	2.69856
H	0.54521	4.65386	1.904
C	1.94389	-5.17587	-0.63999

H	2.69291	-5.66714	-1.26406
C	-4.36414	3.54969	0.84229
H	-4.50357	4.17868	1.72367
C	-1.30661	-3.15379	-4.50797
H	-1.97911	-3.79897	-5.07687
C	5.35693	-2.04169	-1.24157
H	6.15317	-1.78894	-0.53798
C	4.44089	-3.46001	-2.96645
H	4.53207	-4.32062	-3.6326
C	1.01223	3.48038	5.06165
H	0.86856	3.78027	6.10174
C	-3.9794	1.97398	-1.43759
C	1.74225	1.85696	3.43298
H	2.18076	0.88178	3.21688
C	-4.47965	3.27457	-1.53775
H	-4.70823	3.6852	-2.52348
C	-0.86486	-1.95023	-5.05179
H	-1.18994	-1.64803	-6.04958
C	6.10385	-1.80483	2.8264
H	7.15067	-1.82817	3.13636
C	1.32233	-3.31924	0.79257
C	3.41484	1.80637	-5.01487
H	4.25748	1.73495	-5.70572
C	-2.11883	2.34206	2.77348
H	-1.33284	2.03566	2.06539
H	-1.80242	2.0162	3.77627
H	-2.12828	3.44262	2.76814
C	-3.4901	1.77656	2.39252
H	-3.4015	0.68311	2.35787
C	3.15324	-1.57943	-2.1493
C	2.61477	2.94897	-5.00448
H	2.83266	3.77501	-5.68457
C	0.65028	4.34209	4.02796
H	0.22387	5.32136	4.25509
C	-0.26442	-5.098	0.31961
H	-1.25589	-5.53372	0.45922
C	-0.62089	-1.8541	5.54901
H	-1.1517	-1.90056	6.50205
C	-0.76073	-0.74477	4.72237
H	-1.40083	0.08808	5.02089
C	0.74669	-1.73965	3.09756
C	-0.08677	-0.69508	3.50166

H	-0.20433	0.18211	2.86445
C	-4.53181	2.11592	3.46234
H	-4.56902	3.19532	3.67381
H	-4.2827	1.60999	4.40745
H	-5.54132	1.79964	3.16114
C	4.00491	-2.94935	2.45881
H	3.434	-3.87951	2.47376
C	-0.88782	-3.52817	-3.23107
H	-1.22509	-4.46838	-2.79006
C	0.05744	-3.90075	0.95468
H	-0.68533	-3.41938	1.59311
C	1.12956	5.64217	-1.52532
H	1.7584	6.44644	-1.9126
C	5.33974	-2.97203	2.85546
H	5.78725	-3.91082	3.18805
C	0.20303	-2.91093	5.15389
H	0.31619	-3.78666	5.796
C	0.88498	-2.85088	3.94344
H	1.51911	-3.68935	3.65012
C	0.67919	-5.73884	-0.48376
H	0.4305	-6.67875	-0.98064
C	-0.24545	5.66023	-1.74629
H	-0.70169	6.47802	-2.30795
C	-6.84363	0.2861	0.4785
H	-7.36837	-0.23728	-0.33635
H	-6.32047	1.14651	0.03735
H	-7.6176	0.68379	1.15513
C	4.26392	2.97666	1.51617
H	3.81974	3.22277	2.4813
C	-0.44978	3.58798	-0.52945
H	-1.09861	2.80085	-0.13803
C	5.44653	2.38308	-0.93776
H	5.8956	2.15407	-1.90635
C	-4.80656	1.27254	-3.74874
H	-4.88681	2.27434	-4.19797
H	-5.78425	1.02388	-3.309
H	-4.61053	0.56439	-4.56806
C	6.23192	2.85827	0.11202
H	7.30553	3.00231	-0.02554
C	-3.68946	1.192	-2.70708
H	-3.58774	0.14134	-2.42331
C	-1.0385	4.63091	-1.23847

H	-2.11922	4.63	-1.38791
C	-5.90057	-0.65891	1.23979
H	-5.43308	-0.07825	2.05197
C	-3.06098	-2.23739	2.49058
H	-3.95863	-2.24966	3.12726
H	-2.61883	-1.23503	2.58285
H	-2.34143	-2.94361	2.93878
C	-2.34198	1.61697	-3.29708
H	-2.08955	1.01708	-4.18444
H	-1.52798	1.48075	-2.56684
H	-2.33908	2.68121	-3.58149
C	-3.40192	-2.60841	1.04272
H	-2.45306	-2.62682	0.46044
C	5.63535	3.15974	1.3347
H	6.23856	3.54736	2.15841
C	-3.88592	-2.42189	-2.35659
H	-3.57293	-3.40675	-1.9764
H	-2.98622	-1.78519	-2.36224
H	-4.17825	-2.56138	-3.40995
C	-4.68611	4.05842	-0.40938
H	-5.08404	5.07048	-0.50606
C	-6.23978	-2.78972	-1.51936
H	-6.51474	-3.06883	-2.5496
H	-7.12719	-2.33014	-1.06226
H	-6.03407	-3.72423	-0.97587
C	-5.03407	-1.83939	-1.5283
H	-5.36993	-0.90916	-2.01967
C	-6.69135	-1.79555	1.90601
H	-7.50637	-1.38255	2.52226
H	-6.06623	-2.41128	2.56903
H	-7.15513	-2.46925	1.1699
C	-3.96418	-4.03288	0.96703
H	-3.30832	-4.73634	1.50666
H	-4.05536	-4.39217	-0.06746
H	-4.95926	-4.10473	1.43149

4. References

1. (a) I. C. Cai, M. I. Lipschutz, T. D. Tilley, *Chem. Commun.* **2014**, *50*, 13062−13065; (b) I. C. Cai, M. S. Ziegler, P. C. Bunting, A. Nicolay, D. S. Levine, V. Kalendra, P. W. Smith, K. V. Lakshmi, T. D. Tilley, *Organometallics* **2019**, *38*, 1648−1663.

2. A. J. Martínez-Martínez, A. S. Weller, *Dalton Trans.*, **2019**, *48*, 3351–3354.

3. A. J. Sicard, R. T. Baker, *Org. Process Res. Dev.* **2020**, *24*, 2950−2952.

4. M. Muhr, P. Heiß, M. Schütz, R. Bühler, C. Gemel, M. H. Linden, H. B. Linden, R. A. Fischer, *Dalton Trans.*, **2021**, *50*, 9031−9036.

5. G. M. Sheldrick, SHELXL-97, Program for Crystal Strucutre Refinement, Göttingen, 1997.

6. G. Sheldrick, *Acta Crystallogr., Sect. C: Struct. Chem.*, **2015**, *71*, 3-8.

7. M. J. Frisch, G. W. Trucks, H. B. Schlegel, G. E. Scuseria, M. A. Robb, J. R. Cheeseman, G. Scalmani, V. Barone, G. A. Petersson, H. Nakatsuji et al., Gaussian 16 Rev. C.01, Wallingford, CT, 2016.

8. a) A. D. Becke, *J. Chem. Phys*., **1997**, *107*, 8554-8560; (b) F. Weigend, R. Ahlrichs, *Phys. Chem. Chem. Phys.*, **2005**, *7*, 3297-3305; (c) J.-D. Chai, M. Head-Gordon, *Phys. Chem. Chem. Phys.*, **2008**, *10*, 6615-6620; (d) S. Grimme, J. Antony, S. Ehrlich, H. Krieg, *J. Chem. Phys*., **2010**, *132*, 154104.

9. Glendening, E. D., Badenhoop, J, K.; Reed, A. E.; Carpenter, J. E.; Bohmann, J. A.; Morales, C. M.; Landis, C. R.; Weinhold, F. Theoretical Chemistry Institute, University of Wisconsin, Madison, 2013.